Heavy Ion Collisions

Cargèse 1984

Edited by

Paul Bonche
CEN Saclay
Gif-sur-Yvette, France

Maurice Lévy
Université Pierre et Marie Curie
Paris, France

Philippe Quentin
Université de Bordeaux
Bordeaux, France

and

Dominique Vautherin
Institut de Physique Nucléaire
Université de Paris XI
Orsay, France

Plenum Press
New York and London
Published in cooperation with NATO Scientific Affairs Division

57

DYNAMICS OF THE RELATIVISTIC HEAVY ION COLLISIONS

J. Cugnon

Physics Department B5
University of Liège, Sart Tilman
B-4000 Liège 1, Belgium

1. INTRODUCTION

1.1. The domain[1]

The boundaries of the relativistic heavy ion collision domain are loosely defined. Obviously, the lower limit is certainly at an incident beam energy (per nucleon) larger than the highest energy discussed by Prof. M. Lefort in his lectures,[2] about 44 MeV/A. The upper limit separating relativistic and ultrarelativistic collisions (discussed elsewhere by Prof. G. Baym[3]) is even more diffuse.
As a convenient but perhaps not very meaningful guide, we will use the present operating accelerators. The Bevalac has accelerated for now twelve years ions up to Ar from 250 MeV/A to 2.1 GeV/A (which corresponds to a Lorentz factor in the lab frame from $\gamma_{inc} = 1.26$ to 3.23). Very recently Nb and La beams have been accelerated and Au and U beams are going to be exploited in the very near future. The Synchrophasotron at Dubna has the more energetic ions available nowadays : up to 4 GeV/A, but unfortunately, only light ions (up to ^{12}C) are available. In the last months or so, C and O beams have been accelerated in the Saturn machine in Saclay at an energy around 1 GeV/A. The Ganil machine in France and the MSU machine should cover the range between 100 MeV and 400 MeV per nucleon, but they are just starting now. As most of the now available data have been obtained in Berkeley, our purpose here is to discuss the physics in the Bevalac range, with some excursions in the Ganil regime.

1.2. The motivation

The fascinating aspect of the Bevalac experiments is the fact that they offer the opportunity to probe highly excited, dense nuclear matter. The hope was to extract from experimental data the nuclear matter equation of state, i.e. the energy per nucleon of a nuclear extended system at density ρ and at temperature T. Up to now, this relation is known with accuracy for only one point, namely $T = 0$, and $\rho = \rho_0 = 0.17\ fm^{-3}$. Properties in a small domain around this point are carried by the compression modulus K, which is known with a reasonable accuracy. Even more fascinating appear the theoretical speculations of the last few years, which suggest novel phases of hadronic matter. Fig. 1 summarizes the main features of this new development.

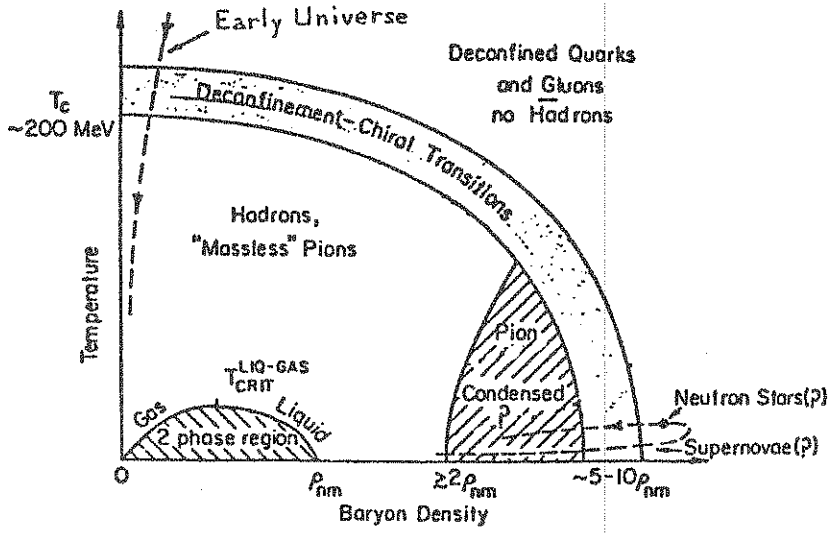

Fig. 1. Phase diagram for hadronic matter, with possible probes of cosmological and astrophysical nature. Adapted from Ref. 3.

At high temperatures and high densities, quarks become deconfined and propagate freely and perhaps loose their mass. Because of spin-isospin long range nuclear forces a pion condensed phase may exist at low temperatures and for $\rho \gtrsim 2\ \rho_0$. At low temperature and for $\rho < \rho_0$, the nuclear matter could exist as a mixture of a gas and a liquid phases. The central part of the diagram would correspond to the ordinary liquid phase of nuclear matter. Some authors make a distinction between nuclear matter as a fluid of neutrons and protons and the hadronic matter which is composed of nucleons, pions (and some other mesons) and Δ's (and some heavier resonances). However, it is likely that mesons and resonances appear progressively and therefore, there is no serious reason to speak of two distinct phases.

The detection of the new phases of matter as well as the determination of the hadronic matter equation of state has appeared as a kind of Holy Grail that the experimentalists around the Bevalac had to quest (this was the only tool to do such a thing if exception is made of some cosmological and astrophysical indications). However, even if gross estimates of densities and temperatures reached during the collision process indicate that exotic phases may be reached, several severe conditions must be fulfilled in such a way that one can speak of a phase transition : (1) the surface effects must not be important ; (2) thermal equilibrium must be realized, at least locally (this term will be discussed later on) ; (3) the compressed matter must live long enough for the transition to take place. None of these requirements are clearly fulfilled in the systems studied up to now, as we will see. Therefore, one can expect to see the onset of critical phenomena only.

From the experimental point of view, only the numerous debris of the often violent reaction are detected. It appears like a formidable challenge to extract from all the complicated patterns of these events (in a streamer chamber experiment, f.i.) any property of the dense system, because (1) the signal is not very well known ; (2) it may take the form of a tiny bump superimposed on a huge background ; (3) final state interaction or experimental bias may distort the signal. Clearly, careful and systematic studies are required as well as a good theoretical guide which provides the basic features of the reaction mechanism. The search for signals has acted as a driving force for both experimentalists and theorists, who in this way have accumulated an impressive amount of new physics, as well as its accompanying amount of deception. We are going to present these new developments in the following chapters.

2. SIMPLE PICTURE: PARTICIPANTS AND SPECTATORS

2.1. Simple classification of events

Global detectors (like streamer chamber) reveal that events can be grossly classified into three types :

(a) peripheral events, which are expected to occur for large impact parameters. In these events, the momentum transfer between the two partners is small and the projectile simply fragments and produces a jet of particles in the forward direction ;

(b) central events, which presumably occur at small impact parameters. These events are violent and a total disintegration of the system results from a large momentum transfer between the two partners ;

(c) events, where the two features coexist : a forward jet is to be seen along with many tracks at large angles.

Counter experiments looking at the emission of protons corroborate these features, as shown in Fig. 2.

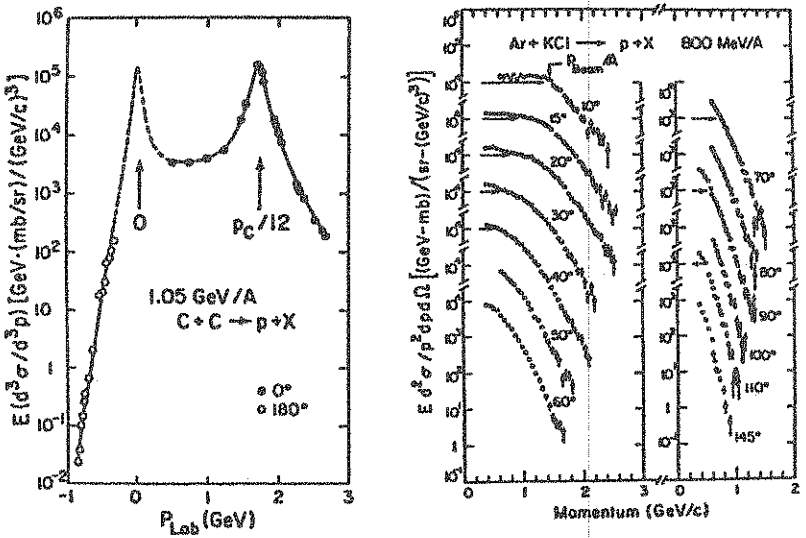

Fig. 2. Left : proton spectrum at 0° and at 180° showing the spectator peaks and the participants in between. Right : proton spectrum at various angles. Adapted from Ref. 4.

Clearly, at 0° protons are detected with an appreciable rate around the velocity of the projectile. A corresponding peak for the target is expected. The particles detected in these peaks are suggestively called spectator particles. The region in momentum space where these particles are detected is named the fragmentation region. At 0° protons with intermediate velocities are detected. They are produced by large momentum transfers. When one gets off the beam direction, they are more and more visible. Those particles are called participants. These observations suggest that in a first approximation the nucleons are behaving independently, like in a gas.

2.2. Characteristic lengths

It is instructive, when tackling a new domain, to look at the characteristic lengths (or times) of the system under study. Often, this helps to build a general frame, which may serve to generate a simplified picture, that is to be improved further and further. In Fig. 3, we have indicated several characteristic lengths and energies. In the Bevalac region, the incident energy per particle is notably larger than both the Fermi energy and the binding energy per particle. Therefore, binding effects as well as Fermi statistics are not expected to play an important role. Because this region is above the threshold, pion production will be an important aspect of the collision process. Along the ordinate axis, we exhibit some characteristic lengths. As can be seen, the range of the nucleon-nucleon (NN) force r_s is smaller than the average inter-nucleon distance d, which in turn is smaller than the radius R of the nuclei.

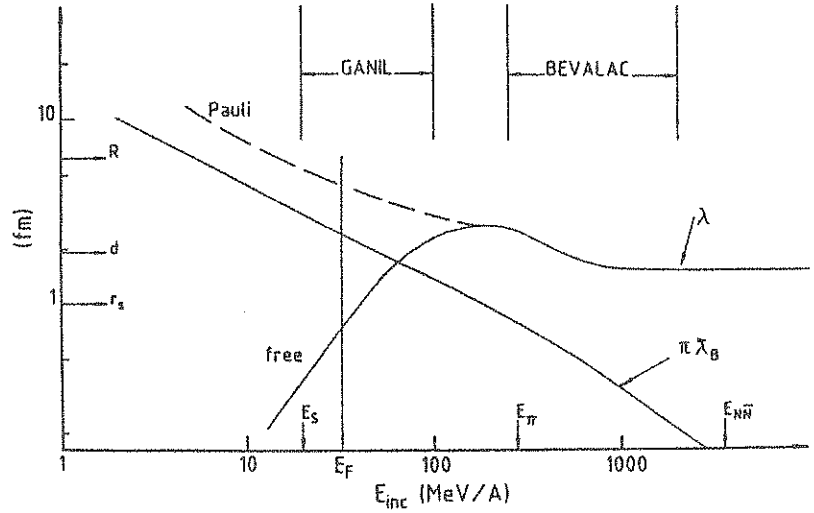

Fig. 3. Typical characteristic lengths and energies for a colliding nucleus-nucleus system. E_π is the threshold for pion production in the NN system. See text for detail.

Another interesting parameter is the de Broglie wave length $\lambda\!\!\!^{-}_{B}$ for the relative NN motion. It is smaller than d in the Bevalac domain. Those parameters are such that the collision processes can be viewed (in a kind of roughly approximate picture) as a succession of independent binary collisions between classical nucleons, although it should be stressed that the strict validity of this picture would rather require $\lambda\!\!\!^{-}_{B}$, $r_s \ll d \ll R$ and not simply "smaller" signs. Also Fig. 3 gives the mean free path λ as calculated in the gas limit (with and without Pauli blocking correction). We will come back on the role of this parameter. Finally, Fig. 3 shows that the Ganil physics could be quite complicated because in this energy domain, many parameters are comparable. In the remaining part of this section, we are going to review all the information that can be extracted from experiment using only this simple picture of successive collisions.

2.3. Role of the geometry

It is now a popular idea that the geometry itself determines the way nucleons are separated into participants and spectators : If a nucleon is in the part of the projectile (target) intercepted by the target (projectile), it will be a projectile (target) participant. If, on the other hand, the nucleon belongs to the outer parts of the system, it will be a spectator. Such a geometrical picture leads to a proton participant cross-section

$$\sigma_p = \pi r_o^2 \, (Z_P \, A_T^{2/3} + Z_T \, A_P^{2/3}) \qquad (2.1)$$

and to a projectile spectator cross-section

$$\sigma_{sp}^{p} = \pi r_o^2 \, (Z_T \, A_T^{2/3} + 2 \, A_P^{1/3} \, A_T^{1/3}) \quad . \qquad (2.2)$$

The mass dependence has been checked experimentally by Nagamiya[4,5] in light to medium-heavy systems. The agreement with Eqs. (2.1-2) is quite good if he used r_o = 1.2 fm for the participants and 0.95 fm for the spectators. The smaller value for the spectators is already indicative of a correction to the simple geometrical picture, because of the finite angle NN scattering. Another expected modification comes from the (limited) transparency of the nuclei, due to finite mean free path.

2.4. Evidence for multiple collisions

The best way to study the properties of the participant region is to look at 90°-c.m. for equal-mass systems, because one is then far from the spectator region. Proton energy spectra at 90° c.m. in several systems is given in Fig. 4. Typical features are observed.

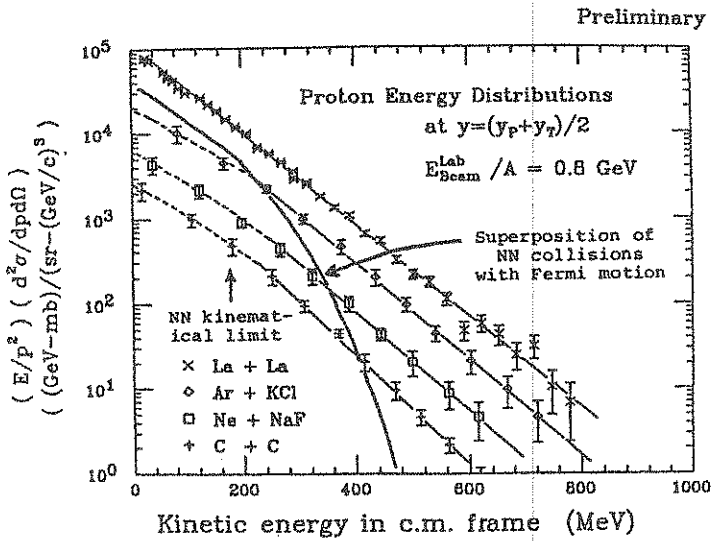

Fig. 4. Proton energy spectrum at 90° in the c.m. frame for various symmetric systems. The full line indicates the kinematical limit obtained by taking account of a reasonable Fermi distribution. Adapted from Refs. 6-7.

First, the spectrum is rather the same for all the systems. This suggests that the relevant quantity is the beam energy per nucleon rather than the total energy. This is in keeping with the idea that the basic mechanism is a superposition of NN collisions. Second, high energy protons are emitted abundantly well beyond the kinematical limit, even if Fermi motion is taken into account. Third, the high energy domain approaches an exponential, with deviations on the low energy side. Fourth, the slope parameter E_o characterizing the exponential shape is quite large : 70-80 MeV. The slope parameter is also increasing with the mass of the system indicating that high energy protons are produced via multiple collisions.

These very simple observations suggest that through multiple collisions, the participant nucleons are spread over the whole momentum space that they have at their disposal (the so-called phase space or thermal limit). This is not true, however, because of two observational facts, which indicate that some nucleons are just making a small number of collisions.

2.5. Evidence for hard scattering

If the thermal limit was attained, the angular distribution would be isotropic in the c.m. of equal mass systems. The experiment shows that it is forward (and backward) peaked, suggesting that some nucleons are making just one or two collisions, since the NN differential cross-section is forward peaked. The presence of such a hard component, as it is named, has been nicely demonstrated in correlation experiments by Nagamiya et al.[8-10]. The idea is to detect a proton at one angle and to look for coincidence with the proton detected in another counter, whose direction may be varied. They observed that the coincidence yield is enhanced when the position of the second counter and the energy of the second proton is such that the two outgoing protons correspond to a possible final state of a proton-proton system with the same velocity as the incoming nuclei. Those protons thus do not interact with the other nucleons. It is understandable that the frequency of such pairs provides a measure of the mean free path λ of nucleons since the probability for a nucleon to do not suffer an additional collision is roughly $\exp(-R/\lambda)$, where R is the radius of the interaction zone. In proton-nucleus interactions, R is well defined, and the experiments lead to a value of $\lambda \simeq 2.4$ fm around 0.8 Gev.[10-11] With this value, one can use the correlation experiments to determine R. The extracted values are consistent with two-pion and two-proton interferometry.

2.6. Pion energy spectra

An important piece of data is the 90° c.m. spectrum of (negative) pions in equal mass systems. They look pretty much exponential (without any shouldering like in the proton case). The

extracted values of the slope parameter E_0 are given for the Ne + NaF system in Fig. 5, along with the proton slope parameter.

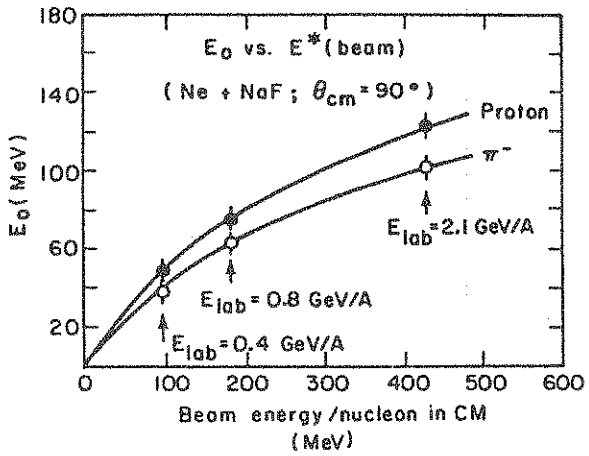

Fig. 5. Values of E_0 for both pions and protons as a function of the beam energy per nucleon in the c.m. frame. Figure taken from Ref. 12.

As expected, E_0 is increasing with the incident energy. In addition, the values for the pions are systematically smaller than the values for the protons. There are several proposed explanations for $E_0(\pi^-) < E_0(p)$, in terms of mean free path,[4] of the importance of the Δ-resonances as a pion source,[13,14] or of blast wave.[15] We will come back to these possibilities. Let us point out here the last explanation, which implies the rapid expansion of the participant system, an expected feature in view of the pressure that can be built if the matter is coming to stop in the c.m. system.

2.7. Summary

All these considerations lead to the following picture, which can be adopted as an organization principle in classifying data and models. The nucleons are separated into participants and spectators in a geometrical way. The spectators are little affected, whereas the participants are spread over the momentum space by the virtue of the two-body collisions. Some are scattered many times, some only once. They are very likely compressed in an early stage and afterwards expand very quickly under the action of the pressure.

3. NON EQUILIBRIUM DYNAMICS

3.1. Quantal and classical aspects

Ideally, the heavy-ion collision should be described by a complete quantum theory of strong interactions, QCD as it is generally believed. Needless to say that this is out of scope for the time being. Even a field theoretical description using point-like nucleons and mesons is hopeless, except in very simplified one-dimensional models. The next less fundamental step is to consider point-like nucleons (we disregard pion production for the presentation) whose interaction can be described in terms of potentials or perhaps in terms of scattering amplitudes or cross-sections. With this starting point of view, various many-body theories are at our disposal, both in the classical and in the quantum regimes. Fig. 6 gives the relationship between these theories.

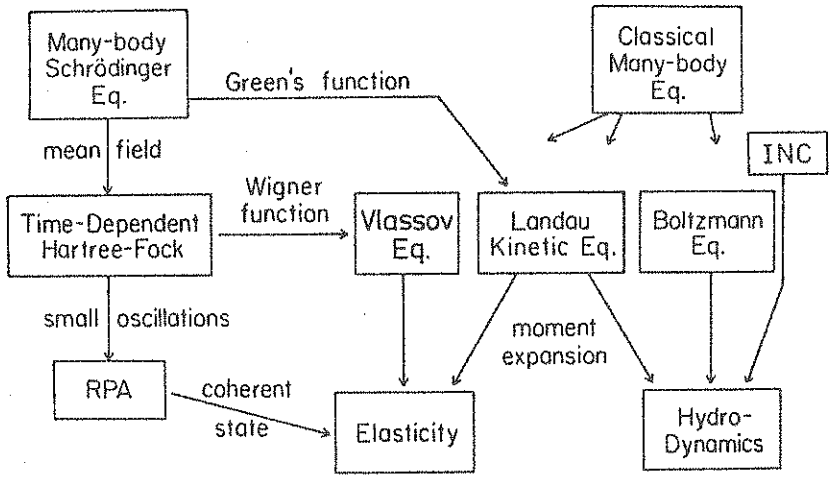

Fig. 6. The relationship between many-body theories. Adapted from Ref. 16.

Although, as we shall see, the most appropriate and tractable theory is the Boltzmann kinetic equation (or rather the closely related cascade model), it is worth to see whether one should start from a classical or a quantal point of view. This question cannot be answered globally and the choice may vary according to the observables and the kinematic domain one is looking at. For instance, the elastic scattering, which accounts for nearly one half of the total cross-section, has a diffractive quantal nature. However, one is much more interested in the reaction cross section,

inclusive or partially exclusive measurements. In these cases, the interference between partial waves is expected to play a secondary role, because of the very many final states. Therefore (and also because the nucleus-nucleus wave number is very large), the classical concept of impact parameter may be used and one may simply sum over impact parameters.

Looking a little bit further at quantum features of the collision path, one realizes that in a nucleon-nucleon (NN) collision, the maximum angular momentum ℓ_{max} is not large : for a relative momentum of 1 GeV/c, $\ell_{max} \approx 3$, if one considers the range of nucleon-nucleon forces. Thence, the NN scattering should in principle be described at a quantum level.

Let us now turn to the possible interference between NN scatterings. Has the scattering wave function reached its asymptotic (far zone) behaviour, before hitting another nucleon ? Two successive scatterings occur *in the average* after a mean free path λ

$$\lambda = \frac{1}{\rho\ \sigma_{NN}} \tag{3.1}$$

The near zone limit is at least the range of the NN force r_s (see Fig. 3). Around 1 GeV/A, $\lambda \approx 1.6$ fm, which is of the same order as the range of the force, and interferences are expected. However, in nucleus-nucleus collisions, so many interferences will occur (compared to proton-nucleus) that, very likely, they will cancel out.

Another quantum effect arises from the fact that during the successive collisions, the particles are off their energy shell. This aspect has been investigated by Danielewicz[17] and can be stated as follows. During two successive collisions the energy of the particle cannot be fixed better than with an uncertainty of $\delta\varepsilon = \hbar/\delta t$, where δt is the time interval separating the collisions. One readily has

$$\frac{\delta\varepsilon}{\varepsilon} \approx \frac{2}{\lambda\ k} \approx \frac{\lambda\!\!\!^{-}_B}{\lambda} \tag{3.2}$$

which is of the order of 25% or less. According to ref. 17, this has profound implications on the equilibration process. It is not clear yet whether this effect differs from the previous one.

Let us finally mention quantum effects linked with quantum statistics, in the depopulation of the Fermi spheres and also in the final state interaction. The latter leads to interference between two protons or two pions, if they have small relative momentum.

3.2. From many-body theory to a kinetic equation

The very first starting point is the many-body Schrödinger equation, if we adopt the quantum point of view. Although, as we will see, a classical approach is largely sufficient around 1 GeV/A, we nevertheless choose this presentation, because it may give contact with the low-energy side. We closely follow the presentation of Ref. 16. The approximation scheme is better described on the A-body density matrix

$$\tilde{\rho}(\vec{r}_1,\ldots\vec{r}_A,\vec{r}'_1,\ldots\vec{r}'_A,t) = \psi^*(\vec{r}_1,\ldots\vec{r}_A,t)\psi(\vec{r}'_1,\ldots\vec{r}'_A,t) \tag{3.3}$$

from which one may define the one-body density matrix

$$\rho^{(1)}(\vec{r},\vec{r}',t) = A \int d^3r_2 \ldots d^3r_A\ \tilde{\rho}(\vec{r},\vec{r}_2\ldots\vec{r}_A,\vec{r}',\vec{r}_2,\ldots\vec{r}_A,t) \tag{3.4}$$

and the two-body density matrix

$$\rho^{(2)}(\vec{r}_1,\vec{r}_2,\vec{r}'_1,\vec{r}'_2,t) = A(A-1) \int d^3r_3\ldots d^3r_A\ \tilde{\rho}(\vec{r}_1,\vec{r}_2,\ldots\vec{r}_A,\vec{r}'_1,\vec{r}'_2,\vec{r}_3\ldots\vec{r}_A,t) \ . \tag{3.5}$$

The equation of motion for $\rho^{(1)}$ is obtained by integrating the Von Neumann equation

$$\frac{\partial\tilde{\rho}}{\partial t} = \frac{i}{\hbar}[H,\tilde{\rho}] \tag{3.6}$$

over all but one coordinates:

$$\frac{\partial\rho^{(1)}}{\partial t}(\vec{r},\vec{r}',t) = -i\,\frac{\nabla^2 - \nabla'^2}{2m}\ \rho^{(1)}$$

$$+ i \int d^3r_2\ (v(\vec{r},\vec{r}_2) - v(\vec{r}',\vec{r}_2))\ \rho^{(2)}(\vec{r},\vec{r}_2,\vec{r}',\vec{r}_2,t) \ . \tag{3.7}$$

The evolution of $\rho^{(1)}_{(2)}$ involves the quantity $\rho^{(2)}$. Analogously, the evolution of $\rho^{(2)}$ involves $\rho^{(3)}$, etc. One so generates a hierarchy of equations, similar to the BBGKY equations[18] for the classical distribution functions, and also to the Martin-Schwinger[19] formalism for the Green functions. The idea is to truncate the hierarchy somewhere to close the set of equations.

It is interesting at this stage to introduce the Wigner transform[20] of the one-body density

$$f_1(\vec{r},\vec{p},t) = \int \frac{d^3s}{(2\pi\hbar)^3}\ e^{\frac{i}{\hbar}\vec{p}.\vec{s}}\ \rho^{(1)}(\vec{r}+\frac{\vec{s}}{2}\ ,\ \vec{r}-\frac{\vec{s}}{2},\ t) \ . \tag{3.8}$$

This Wigner function behaves in many ways as the classical one-body distribution function (we will use the same symbol to designate the two quantities). In particular the particle density ρ, the particle current $\vec{j}$ and the momentum tensor are given by the same integrals

$$\rho(\vec{r},t) = \rho^{(1)}(\vec{r},\vec{r},t) = \int d^3p\ f_1(\vec{r},\vec{p},t) \qquad (3.9)$$

$$\vec{j}(\vec{r},t) = \frac{1}{m}\{(\frac{\vec{\nabla} - \vec{\nabla}'}{2i})\ \rho^{(1)}(\vec{r},\vec{r}')\}_{\vec{r}=\vec{r}'} = \int d^3p\ \frac{\vec{p}}{m}\ f_1(\vec{r},\vec{p},t) \qquad (3.10)$$

$$\tau_{ij}(\vec{r},t) = \int d^3p\ p_i\ p_j\ f_1(\vec{r},\vec{p},t) \quad . \qquad (3.11)$$

The main difference is that the Wigner function is not necessarily non-negative. Similarly, one can define the analog of the two-body distribution function

$$f_2(\vec{r}_1,\vec{r}_2,\vec{p}_1,\vec{p}_2,t) = \int \frac{d^3s_1}{(2\pi\hbar)^3}\frac{d^3s_2}{(2\pi\hbar)^3}\ e^{\frac{i}{\hbar}(\vec{p}_1.\vec{s}_1 + \vec{p}_2.\vec{s}_2)}$$

$$\rho^{(2)}(\vec{r}_1 + \frac{\vec{s}_1}{2},\ \vec{r}_2 + \frac{\vec{s}_2}{2},\ \vec{r}_1 - \frac{\vec{s}_1}{2},\ \vec{r}_2 - \frac{\vec{s}_2}{2},\ t) \quad . \qquad (3.12)$$

Using Eq. (3.8), Eq. (3.7) can be put the form

$$\frac{\partial}{\partial t} f_1 + \frac{\vec{p}}{m}.\vec{\nabla} f_1 = i \int \frac{d^3\vec{x}}{(2\pi)^3}\ e^{\frac{i}{\hbar}\vec{p}.\vec{x}} \int d^3r'' \times$$

$$[v(\vec{r} + \frac{\vec{x}}{2},\ \vec{r}'') - v(\vec{r} - \frac{\vec{x}}{2},\ \vec{r}'')]\ \rho^{(2)}(\vec{r} + \frac{\vec{x}}{2},\ \vec{r}'',\ \vec{r} - \frac{\vec{x}}{2},\ \vec{r}'',t) \qquad (3.13)$$

or

$$(\frac{\partial}{\partial t} + \frac{\vec{p}}{m}.\vec{\nabla})f_1 = i \int \frac{d^3\vec{x}}{(2\pi)^3}\ e^{i\vec{p}.\vec{x}} \int d^3r'' \times$$

$$[v(\vec{r}+\frac{\vec{x}}{2},\vec{r}'') - v(\vec{r}-\frac{\vec{x}}{2},\vec{r}'')] \int d^3p_1\ e^{-i\vec{p}_1.\vec{x}} \int d^3p_2\ f_2(\vec{r},\vec{r}'',\vec{p}_1,\vec{p}_2,t) \qquad (3.14)$$

This equation is not very useful since it cannot be solved exactly. So we turn to its usual approximations. The factorization of $\rho^{(2)}$ into two one-body density matrices

$$\rho^{(2)}(\vec{r}_1,\vec{r}_2,\vec{r}'_1,\vec{r}'_2,t) = \rho^{(1)}(\vec{r}_1,\vec{r}'_1,t)\ \rho^{(1)}(\vec{r}_2,\vec{r}'_2,t)$$

$$- \rho^{(1)}(\vec{r}_1,\vec{r}'_2,t)\ \rho^{(1)}(\vec{r}_2,\vec{r}'_1,t) \qquad (3.15)$$

closes the equation (3.13) on itself as an equation for f_1. Retaining the first term in Eq. (3.15) leads to the Hartree approximation which may be written as

$$[\frac{\partial}{\partial t} + \frac{\vec{p}}{m}.\vec{\nabla} - (\vec{\nabla}U).\vec{\nabla}_{\vec{p}}]\ f_1(\vec{r},\vec{p},t) = 0 \quad , \qquad (3.16)$$

where U is the Hartree potential

$$U(\vec{r}) = \int v(\vec{r} - \vec{r}')\ \rho^{(1)}(\vec{r}',\vec{r}')d^3r' \quad , \qquad (3.17a)$$

or

$$U(\vec{r}) = \int d^3r'\ d^3p\ v(\vec{r} - \vec{r}')\ f_1(\vec{r}',\vec{p},t) \quad . \qquad (3.17b)$$

This equation, obtained by retaining the first order term in the expansion of the bracket in (3.13) as a power series of $\vec{x}$, (this amounts to assume that the potential is a smooth function) is formally the same as the Liouville equation for free particles in an external potential. The new feature here is that U is generated by the particles themselves and is density dependent : it is known as the *Vlassov* equation. Except for this density dependence, the equation conserves density in phase space, and does not contain expected non-equilibrium effects.

The Hartree-Fock approximation, which leads to the well-known TDHF formalism gives rise to a complicated equation in phase space. The dynamics implied by this equation is essentially the same as the one of the Vlassov equation once a Slater determinant has been chosen as a starting point for the latter. It is generally designated as the one-body dynamics and is extensively covered in Refs. 21.

The one-body distribution function is influenced by collisions also. The effect of the latter is introduced by higher order approximation. Such a program has been carried out within the formalism of the Green's functions by Kadanoff and Baym[22]. We merely quote the result here, which is an equation of the form

$$[\frac{\partial}{\partial t} + \frac{\vec{p}}{m}.\vec{\nabla} - (\vec{\nabla}U).\vec{\nabla}_p]\ f_1(\vec{r},\vec{p},t) =$$

$$\int \frac{d^3p_2}{2\pi}\frac{d^3p_3}{2\pi}\frac{d\,p_4}{2\pi} W(\vec{p}_3\vec{p}_4 \to \vec{p}\vec{p}_2)\,\delta^3(\vec{p})\,\delta(E) \times$$

$$[\tilde{f}_3\tilde{f}_4(1-\tilde{f})(1-\tilde{f}_2) - \tilde{f}\tilde{f}_2(1-\tilde{f}_3)(1-\tilde{f}_4)] \qquad (3.18)$$

where

$$\tilde{f}_i = f_1(\vec{r},\vec{p}_i,t)/(2\pi\hbar)^3 \qquad (3.19)$$

and where W is a transition rate for collisions between particles of initial momenta $\vec{p}_3$, $\vec{p}_4$ and final momenta $\vec{p},\vec{p}_2$. The delta functions in (3.18) stand symbolically for the conservation laws. This equation is known as the *Landau* equation. In Ref. 22, this result is obtained in a power series expansion in term of the interacting potential v. In this case

$$U = \int d^3r'\, d^3p'\, v(\vec{r}-\vec{r}')f_1(\vec{r}',\vec{p}',t) \qquad (3.20a)$$

$$W(p_3p_4 \to pp_2) = \frac{1}{2}[v(\vec{p}-\vec{p}_3) - v(\vec{p}_2-\vec{p}_4)]^2 \quad . \qquad (3.20b)$$

We have to say that we considerably simplify the presentation here, neglecting aspects like off-shell behaviour, local approximation, etc. We think however that the basic features are preserved.

In the nuclear case, the interacting potential is so strong that, even in a dilute system, the expansion in terms of v breaks down. The usual argument is that, in that particular case, two colliding particles interact repeatedly with each other like in a usual free scattering case. Therefore, it is then more plausible to use

$$U = 0 \qquad (3.21a)$$

$$W(p_3p_4 \to pp_2) = |\langle p_3p_4\ |T|\ pp_2\rangle|^2 \quad , \qquad (3.21b)$$

where T is the usual T-matrix. Whether the two heavy ion system is sufficiently dilute is still an open question. Eq. (3.18) with the choice (3.21) is denoted as the Boltzmann equation. More precisely, this is the (non-relativistic) Uehling-Uhlenbeck equation which becomes the Boltzmann equation when the $(1-\tilde{f})$ factors are removed in Eq. (3.18).

3.3. The intranuclear cascade model (INC)

The intranuclear cascade model is based on a simulation of the collision events. The method presents the great advantage of being capable of handling problems with a large number of degrees of freedom (up to several hundreds) at a microscopic level.

The model describes the collision process as a succession of classical *binary* collisions between *on-shell* particles proceeding *as in free space*. We will not describe it here into detail (see Ref. 23 for that and for a comparison between the various approaches) It is sufficient to say that the particles are given randomly initial positions and momenta consistent with the nuclear density, Fermi motion and incident beam energy. The particles are travelling along straight line trajectories until a pair of them reaches its minimum distance of approach d_{min}. If

$$d_{min} \leq \left(\frac{\sigma_{tot}}{\pi}\right)^{\frac{1}{2}} \quad , \qquad (3.22)$$

where σ_{tot} is the total cross-section, the particles are forced to scatter. The final momenta of the particles are determined by energy-momentum conservation laws and by choosing the scattering angle at random according to a distribution law derived from the experimental differential cross-section. If several channels are open, the final state is chosen at random according to the weights of the respective cross-sections. The straightline motion is then resumed until another pair reaches its minimum distance of approach, etc. The procedure is repeated to obtain a sufficient statistic . Observables and other physical quantities are obtained by ensemble averages. Several features are added like pion production (see later), relativistic kinematics, Pauli blocking, etc.

A widely spread opinion is that INC calculations are just a numerical trick to solve the Boltzmann equation. To support this statement, one invokes the conditions of validity which are roughly the same for the two approaches.

The conditions of validity of the Boltzmann equation are not a trivial matter. They are, however, established heuristically in many textbooks. We follow here Ref. 24. First of all, the basic assumption is that there exists an interval Δt such that

$$\tau_c \ll \Delta t \ll \tau_r \quad , \qquad (3.23a)$$

where τ_c is the (elementary) collision time and τ_r the relaxation time. This condition is easy to understand : one cannot look for variations over characteristic times which are too short since one has neglected the change in the system when the trajectories of the particles are different from a straight line. On the other hand the relaxation of the system, i.e. the evolution of strong local inhomogeneities, cannot be described by derivatives if the relaxation time is too short. The condition (3.23a) is often stated as a low density condition (which may not be strictly equivalent)

$$r_s^3 \rho \ll 1 \quad . \tag{3.23b}$$

Physically, the latter condition ensures that the successive collisions are well separated in space-time.

In deriving the Boltzmann equation, one implicitly assumes that the distribution function does not change significantly over the time interval Δt. In other words, one assumes that the Boltzmann equation is local in time. Similarly, one also neglects space variation of the distribution function over lengths $\Delta \ell$, typical of the distance travelled by the particles during the time Δt : the equation is local in space.

Finally, the factorization

$$f_2 = f_1 f_1 \tag{3.24}$$

is required : this is the celebrated "Stosszahlansatz" or "molecular chaos" assumption, which introduces irreversibility as is well known.

Much less stringent assumptions are required for the INC picture to be correct. Since one does not deal with time derivative, one needs not worry about a characteristic interval Δt smaller than the relaxation time. Only condition (3.23b) is required. The very structure of the INC calculation is not subject to conditions on locality in space-time. Finally, whether a two-body collision occurs or not depends in the INC picture on the probability of finding two nucleons at sufficiently close points with an appropriate relative momentum, a quantity which has something to do with the two-body distribution function f_2. Therefore, two-body correlations effects are really taken into account. Three-body and higher correlations are neglected, as in Boltzmann equation.
In conclusion, it can be said that the INC model goes beyond the Boltzmann equation and beyond the Landau equation as far as the collision term is concerned. Furthermore, the INC is a theory for the evolution of the one-body distribution function, but also of the two, three, ... A-body distribution functions. This is equivalent to say that the INC can predict event-to-event fluctuations

3.4. Classical many-body equations

The heavy ion case has been studied through the so-called equations of motion approach.[25-30] The latter consists in solving the Hamilton equations for A nucleons interacting through central repulsive short-ranged plus attractive long-ranged potentials. This method, which seems to be more fundamental than a kinetic equation (Landau, Boltzmann, INC, ...) presents some technical difficulties : non-physical solutions at low energy, proper choice of the nucleon-nucleon potential, introduction of pion production and large computation times compared to INC. Moreover, the relative motion of two colliding nucleons is treated completely classically, which seems very doubtful in view of what we have said in Section 3.1. This may be important for the evolution in phase space. On the other hand, the equation of motion approach can incorporate two-body interaction energy, contrarily to a kinetic equation approach.

3.5. Moment expansion of the Landau equation

For the Boltzmann and Landau equations, there are five and only five conserved quantities (called the collisional invariants) :

$$I_n = \int d^3r \, d^3p \, \gamma_n \, f_1(\vec{r},\vec{p},t) \quad , \tag{3.25}$$

with

$$\gamma_n = 1, \ \vec{p}, \ p^2 \quad . \tag{3.26}$$

The conservation laws may be written in a local form by taking the lowest moments in $\vec{p}$ of the Landau equation (3.18). The zeroth moment yields (with (3.9-10), and assuming a finite system) the equation of continuity

$$\frac{\partial \rho}{\partial t} + \vec{\nabla}.\vec{j} = 0 \quad , \tag{3.27}$$

or

$$\frac{\partial \rho}{\partial t} + \vec{\nabla}.(\rho\vec{u}) = 0 \quad . \tag{3.28}$$

The last equation defines $\vec{u}$, the average macroscopic velocity. The first moment gives (with Eq. (3.11))

$$m \frac{\partial \vec{j}}{\partial t} + \vec{\nabla}.\underset{\approx}{\tau} + \rho \, \vec{\nabla} \, U = 0 \tag{3.29}$$

or

$$m \frac{\partial \vec{j}}{\partial t} + \vec{\nabla}.\underset{\approx}{\tau} + \vec{\nabla}(\rho U - V) = 0 \quad , \tag{3.30}$$

where

$$V[\rho] = \int_0^\rho U(\rho') \, d\rho' \quad . \tag{3.31}$$

Equation (3.30) may be rewritten in terms of $\vec{u}$. One readily gets

$$\rho[\frac{\partial \vec{u}}{\partial t} + \vec{u}.\vec{\nabla} \, \vec{u}] + \vec{\nabla}.\underset{\approx}{\Pi} = 0 \tag{3.32}$$

where

$$\Pi_{ij} = S_{ij} + \delta_{ij}(\rho U - V) \quad . \tag{3.33}$$

The quantity

$$S_{ij} = m^2 \int d^3p \ \delta v_i \ \delta v_j \ f_1(\vec{r},\vec{p},t) \qquad (3.34)$$

where $\delta\vec{v}$ is defined by

$$\vec{p} = m(\vec{u} + \delta\vec{v}) \quad , \qquad (3.35)$$

is the momentum tensor in the matter (local) rest frame. The quantity Π is the momentum flux tensor.

The second moment equation is obtained, after some tedious algebra. It reads

$$(\frac{\partial}{\partial t} + \vec{u}.\vec{\nabla})\ S_{ij} = -\sum_k (S_{ik}\ \nabla_k\ u_j + S_{jk}\ \nabla_k\ u_i) - S_{ij}\ \vec{\nabla}.\vec{u}$$

$$- m\ \vec{\nabla}.\vec{J} + m \int I\ \delta v_i\ \delta v_j\ d^3p \quad . \qquad (3.36)$$

In this equation, $\vec{J}$ is the internal energy current

$$\vec{J} = \int d^3p\ \frac{(\vec{p} - m\vec{u})^2}{2m} (\frac{\vec{p}}{m} - \vec{u})\ f_1(\vec{r},\vec{p},t) \quad , \qquad (3.37)$$

and I stands symbolically for the collision term of the Landau equation. Defining the energy density by

$$\rho\ e(\vec{r},t) = \int d^3p\ \frac{p^2}{2m}\ f_1(\vec{r},\vec{p},t) - \frac{1}{2}\rho\ u^2 = \frac{1}{2}\ tr\ \underset{\approx}{S} \quad , \qquad (3.38)$$

one obtains

$$\rho[\frac{\partial}{\partial t} + \vec{u}.\vec{\nabla}]e + \vec{\nabla}.\vec{J} = -\sum_i \sum_k S_{ik}\ \nabla_k\ u_i \quad . \qquad (3.39)$$

The collision term contribution in (3.36) vanishes when the trace is taken.

One generally wants to close the moment equations. This is usually done phenomenologically, as in hydrodynamics. We postpone the discussion of this case to Section 5. We will show here that the long relaxation time limit gives the elasticity limit. Indeed, if a uniform damping due to the collision term is assumed,

$$m \int I\ \delta v_i\ \delta v_j\ d^3p \approx -\frac{(S_{ij} - \frac{1}{3}\delta_{ij}\ tr\ \underset{\approx}{S})}{\tau} \quad , \qquad (3.40)$$

where τ is the relaxation time, Eq. (3.36) can be written, assuming no energy current ($\vec{J} = 0$),

$$(\frac{\partial}{\partial t} + \vec{u}.\vec{\nabla})S_{ij} + \tau^{-1}(S_{ij} - \frac{1}{3}\delta_{ij}\ tr\ \underset{\approx}{S}) =$$

$$-\sum_k (S_{ik}\ \nabla_k\ u_j + S_{jk}\ \nabla_k\ u_i) - S_{ij}\ \vec{\nabla}.\vec{u} \quad . \qquad (3.41)$$

In the long relaxation time limit, the second term may be neglected. By using the notation

$$\frac{D}{Dt} = \frac{\partial}{\partial t} + \vec{u}.\vec{\nabla} \quad , \qquad (3.42)$$

the derivative of (3.32) gives

$$\frac{D}{Dt}\ (\rho\ \frac{D}{Dt}\ \vec{u}) + \frac{D}{Dt}\ \vec{\nabla}.\{S_{ij} + \delta_{ij}(\rho U - V)\} = 0 \quad . \qquad (3.43)$$

Using (3.41), we may write

$$\frac{D}{Dt}\ (\rho\ \frac{D}{Dt}\ \vec{u}) - \vec{\nabla}.\{\sum_k (S_{ik}\ \nabla_k\ u_j + S_{jk}\ \nabla_k\ u_i) + S_{ij}\ \vec{\nabla}.\vec{u}\ \}$$

$$+ \vec{\nabla}\ \frac{D}{Dt}\ (\rho\ U - V) = 0 \qquad (3.44)$$

Now, if we assume that S_{ij} is close to its equilibrium value

$$S_{ij} = \delta_{ij}\ \rho\ \frac{\langle v^2\rangle}{3} \quad , \qquad (3.45)$$

one has

$$\frac{D}{Dt}\ (\rho\ \frac{D}{Dt}\ u_j) - \sum_i \nabla_i\{\rho\ \frac{\langle v^2\rangle}{3}\ (\nabla_i\ u_j + \nabla_j\ u_i) + \vec{\nabla}.\vec{u}\ \}$$

$$- \nabla_j\{\rho^2\ \frac{\partial U}{\partial \rho}\ \vec{\nabla}.\vec{u}\} = 0 \quad . \qquad (3.46)$$

This is the classical equation for vibrations in a solid state which is ordinarily written in terms of displacements

$$\rho\ \frac{\partial^2\ d_i}{\partial t^2} + \lambda\ \nabla_i(\vec{\nabla}.\vec{d}) + \mu \sum_j \nabla_j(\nabla_i\ d_j + \nabla_j\ d_i) = 0 \quad . \qquad (3.47)$$

The Lamé coefficients are

$$\mu = \frac{1}{3}\rho\ \langle v^2\rangle \quad , \quad \lambda = \frac{1}{3}\ \rho\langle v^2\rangle + \rho^2\ \frac{\partial U}{\partial \rho} \quad . \qquad (3.48)$$

This limit is not useful for the heavy ion case. We just give it for the sake of completeness. In heavy ion physics, one is probably closer to the short relaxation time limit, which leads to usual hydrodynamics, as indicated in Fig. 6.

4. EVOLUTION IN PHASE SPACE

4.1. Introduction

The kinetic theories that we have studied in the previous chapter describe the evolution of the system in phase space. However, only the asymptotic properties of the system are measured, f.i. the momentum of the particles. One thus may be interested in the evolution of the system in momentum space only. In Section 4.2, we will investigate this question in some detail. In Section 4.3, we will discuss several aspects of the evolution of the system in phase space. Finally, Section 4.4 will contain a small discussion of the concept of freeze-out as seen from a kinetic point of view.

4.2. Evolution in momentum space

Many models have been proposed to study this aspect. Randrup[31] has studied the Uehling-Uhlenbeck equation (Eq. (3.18)) without convection and potential terms in an homogeneous medium. The r-dependence may be integrated out and the model is applied to two uniform infinite media in relative motion. This may help to look at the equilibration process. However, as Fig. 7 shows, the latter is very much influenced by geometrical properties.

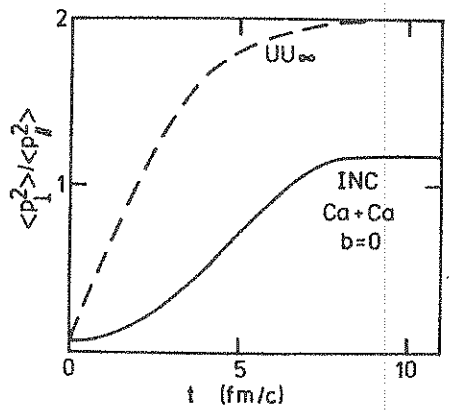

Fig. 7. Comparison of the equilibrium process as predicted by a uniform medium calculation[31] (dotted line) and a 3-dimensional INC calculation[13] (full line) : time evolution of the ratio between average squared longitudinal and perpendicular particle momentum.

The equilibration is much less rapid with real finite nuclei. In the latter case, binary collisions are drastically reduced because of surface and finite size effects. Furthermore, thermalization is not achieved because the system desintegrates rapidly. Let us remind

work of Ref. 31 also shows that the thermalization process is rendered much more efficient by the possible Δ-production. The latte transforms the longitudinal kinetic energy into mass energy and helps to populate the so-called midrapidity region,[13,31] whereas elastic scattering starts to populate the elastic circle (see Fig. 8

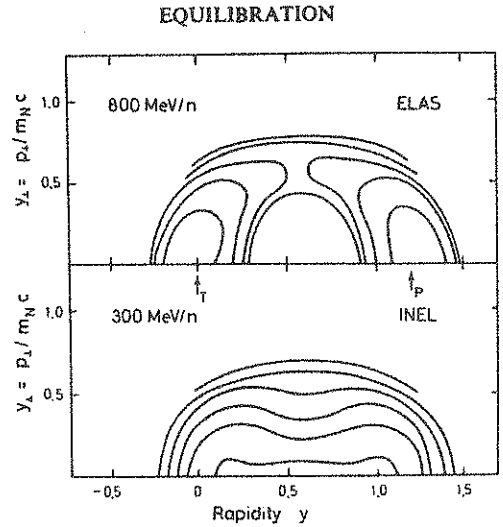

Fig. 8. Contour plots of the distribution of nucleons in rapidity space after their first collision when only elastic NN collisions are considered (upper part, maxima close to the arrows) and when Δ-production is introduced (lower part, maximum close to the $y_\perp = 0$ axis). From Ref. 31.

The features of the final momentum distribution are also interesting to analyze in terms of the number of collisions n undergone by the nucleons. There are numerous models which are dedicated to this study. Let us only mention here the diffusion model of Pirner and Schrürmann[32,33,34] and the closely related approach of Malfliet based on a linear approximation of the Boltzmann equation in momentum space.[35,36] Before entering into the discussion, we make the connection with the experimental data. The invariant nucleon production cross-section can be written as

$$E \frac{d^3\sigma}{dp^3} = \int_0^{b_{max}} 2\pi b\, db \int d^3r\, E\, f_1(\vec{r},\vec{p},b,t) \quad , \qquad (4.1)$$

where we have made explicit the impact parameter dependence of f_1. The quantity b_{max} is the maximum impact parameter ($\approx R_1 + R_2$). The integral (4.1) is time-independent, since for freely moving

$$f_1(\vec{r},\vec{p},t) \approx f_o(\vec{r} - \frac{\vec{p}}{m} t) \quad . \qquad (4.3)$$

We may write the following expansions in terms of n, disregarding the spectators ($n \geq 1$) :

$$\nu = \int d^3r\, d^3p\, f_1(\vec{r},\vec{p},b,t) = \sum_{n\geq 1} f(n) \qquad (4.4)$$

where ν is the number of participants, and

$$(E \frac{d^3\sigma}{d p^3}) = \sum_{n\geq 1} (E \frac{d^3\sigma}{d p^3})_n \quad , \quad \sigma_n = \int \frac{d^3 p}{E} (E \frac{d^3\sigma}{d p^3})_n \quad . \qquad (4.5)$$

Of course, the terms in Eq. (4.5) are not observable quantities, but it is instructive to look at them in the frame of a specific model. Figure 9 shows the quantities entering into Eqs. (4.4-5) as calculated by an INC calculation.[37] The striking feature is the wide distribution of the collision frequencies for central as well as inclusive (integrated over b) collisions. In the average, for central collisions, the nucleons are making 2.78 and 3.24 collisions, for Ne + Ne and Ca + Ca, respectively (~ 4 for Nb + Nb at 400 MeV/A). However, a non negligible number of them are making one collision only.

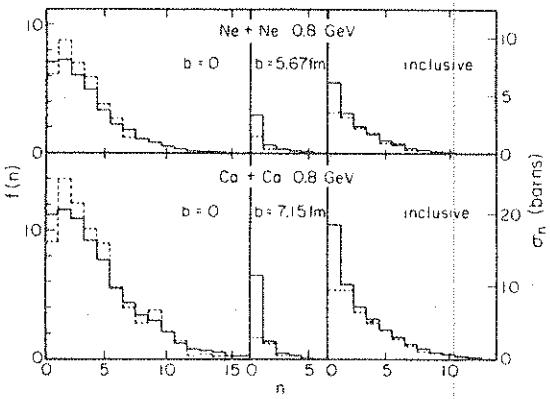

Fig. 9. Quantities f(n) for two impact parameters (left scale) and σ_n (right scale) (Eqs. (4.4-5)), as calculated in Ref. 37. The full lines refer to the final nucleons whereas the dotted lines refer to Δ-particle (× 8).

The spectra are very different according to the number n. They are displayed in Fig. 10, for the Ca + Ca system. For n = 1, the so-called single-scattering component,[38,39] the spectrum is largely dominated by the differential NN cross-section, which is rather well forward-peaked (see also Fig. 8). As n is increasing the central rapidity region fills up whereas the projectile rapidity region is depleted. For n larger than 3, the distribution is close to an isotropic exponentially decreasing (in energy) distribution.

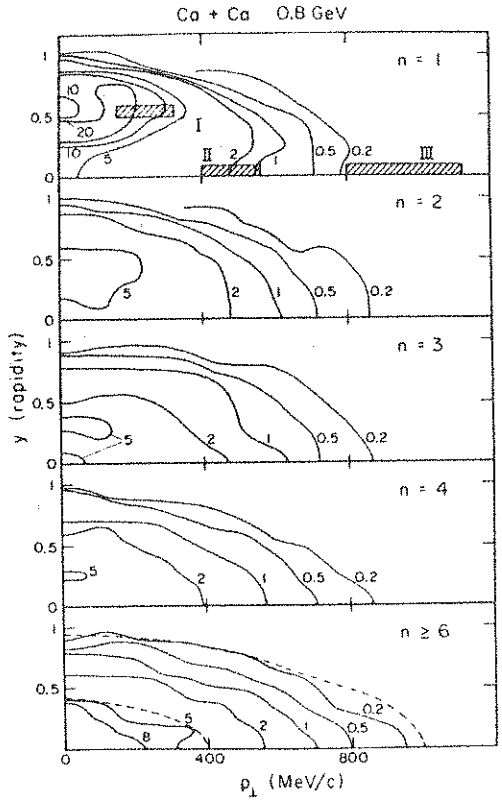

Fig. 10. Invariant cross sections to produce a proton after n collisions as a function of the c.m. perpendicular momentum $p_\perp$ and c.m. rapidity y. They are given in units of 0.462×10^4 mb c^3 GeV^{-2}. Only one half of the rapidity space is shown. To give an idea of the isotropy $n \geq 6$, curves of equal total energy of 1020 and 1371 MeV (dotted curves) have been drawn. Taken from Ref. 37.

As a consequence, only a part of the system may be considered as thermalized (or thermal-like), whereas the remaining nucleons are making few collisions. The importance of the latter part is directly related to the size of the system (and also to the energy) and is decreasing with increasing mass. Let us also mention that the analysis based on the interaction cluster model[40-43] or the so-called phase space model[44-46] leads to the same conclusion, namely that only a part of the system may be considered as equilibrated.

4.3. Evolution in phase space

It is customary to show matter density distribution. We will not do it here because, as we have seen , it is very likely that the equilibrium is not reached. The interested reader may look at Refs. 13, 47, 48, 49. It is however interesting to look at the evolution of the gross properties of the system in phase space. The latter may be conveniently characterized by the second moments of the one-body distribution functions

$$M_{ij}(t) = \int d^3r\, d^3p\, \xi_i\, \xi_j\, f_1(\vec{r},\vec{p},t) \quad , \tag{4.6}$$

where the six-dimensional vector ξ is

$$\xi = \{\vec{r},\vec{p}\} \quad . \tag{4.7}$$

They are 21 of them describing the spatial and momentum extensions of the system, as well as the possible r-p correlations. Some of them are given in Fig. 11.

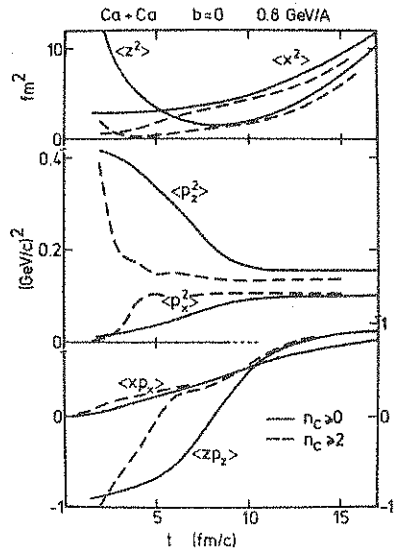

Fig. 11. Time evolution of various moments of the one-particle distribution function f_1. The non diagonal moments $\langle xp_x\rangle$ and $\langle zp_z\rangle$ have been normalized by dividing by $(\langle x^2\rangle\langle p_x^2\rangle)^{\frac{1}{2}}$ $(\langle z^2\rangle\langle p_z^2\rangle)^{\frac{1}{2}}$, respectively. z stands along the beam axis. The full lines correspond to taking all the particles, whereas the dotted lines amount to selecting those that made two collisions at least. Adapted from Ref. 50.

The latter, as well as Fig. 12, gives the result of an INC calculation. It shows that the collision process may be roughly divided into two stages : a compression stage and an expansion stage. At the end of the compression stage, the system is longitudinally compressed into a pancake shape. The transformation of the longitudinal motion into random motion (central part of Fig. 11) goes on a little bit further, although it is not complete, as we have repeatedl said. As time proceeds, the shape of the system becomes more and more

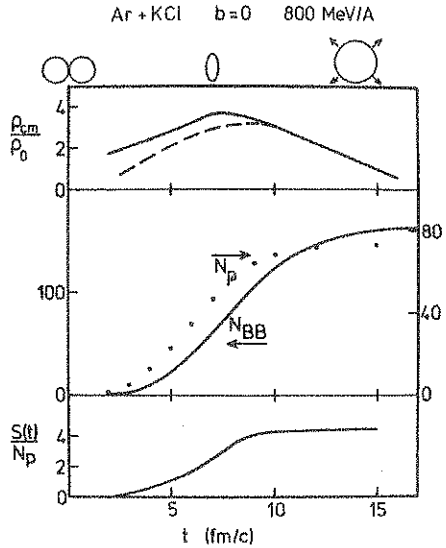

Fig. 12. Time evolution of the baryon density (dashed line : participants only, full line : all baryons included) normalized to the normal density of nuclear matter (top), of the number of baryon-baryon collisions (centre, scale on the left), of the number of participants (centre, scale on the right), and of the entropy of the participant system divided by the final number of participants (bottom). Taken from Ref. 50.

The evolution of the system reveals interesting and complicated features. Figure 12 shows that the system (more precisely the participants in the system) gains entropy during the compression stage. We recall that the entropy per baryon is related to the one-particle distribution function by

$$\frac{S}{A} = 1 - A^{-1} \int d^3r\, d^3p\, f_1(\vec{r},\vec{p},t)\, \ell n\, [f_1(\vec{r},\vec{p},t)(2\pi\hbar)^3] + 4\, \ell n\, 2 \tag{4.8}$$

or, roughly, by

$$\frac{S}{A} \approx 1 - \ell n\, [\bar{f}_1(2\pi\hbar)^3] + 4\, \ell n\, 2 \tag{4.9}$$

if the distribution function is sufficiently close to a constant over the available phase space. The term 4 ℓn 2 enters into (4.8)

because we have assumed spin-isospin degeneracy. The bracket is in some sense the average number of nucleons per natural unit in phase space. After t ≈ 8 fm/c, the system expands at constant entropy. The gain in entropy from configuration space is compensated in momentum space. But this compensation lasts a small time span. After ~ 10-11 fm/c, the system is still expanding, but the momentum distribution does not change anymore (see Fig. 11). We face then a free expansion characterized by a strong correlation between position and momentum. In fact, the behaviour of the xp_x and zp_z correlations allows to consider the system as a more or less globally equilibrated system, i.e. with little correlations, during a very short time interval, say from 7 to 9 fm/c. The situation looks a little bit better for the baryons which are making more than one collision. This is in keeping with what we have noticed at several places.

Let us mention before closing this section, that entropy of the order 4.4 as calculated by the INC calculation corresponds to a fermion-occupancy in phase space of the order 1/10 per unit volume. We will come back to the entropy when discussing deuteron production.

4.4. The freeze-out

By this, one generally means a sudden disappearance of the interaction between particles, which makes an abrupt transition between an expanding system in thermal equilibrium and a freely expanding system. It is reasonable to consider that the freeze-out takes place when the mean freepath λ is equal to the mean distance d between particles. The latter quantity is related to the density ρ by

$$d \approx \rho^{-1/3} \quad . \tag{4.10}$$

Therefore, the freeze-out occurs for

$$\rho = \rho_{fo} \approx \left(\frac{1}{\sigma_{NN}}\right)^{3/2} \quad . \tag{4.11}$$

After the maximum compression (see Fig. 11), the average energy is such that σ_{NN} ~ 20 mb, which makes $\rho_{fo} \approx 2\ \rho_o$. This seems quite a large value. However, we see in Fig. 11 that it is approximately the point beyond which the $\vec{r}.\vec{p}$ correlations are growing considerably. This is just what we expect in a simple-minded picture of the freeze-out as examplified in Fig. 13 for the one-dimensional case. During the isoentropic expansion, the system expands in staying in a thermal equilibrium state : without any $\vec{r}.\vec{p}$ correlations, and keeping the same phase space extension. The box in Fig. 13 increases along the r-axis and shrinks correlatively along the p-axis. After the freeze-out, the box is distorted by the free expansion of the system and $\vec{r}.\vec{p}$ correlations are building up. The calculation shown in Fig. 11 seems to follow this pattern with some deviations however. The binary collisions seem to persist after the $\vec{r}.\vec{p}$ correlations presumably comes from fluctuations in the internucleon distance and the non-uniformity of the density. In addition, the expansion prior to freeze-out (from t ≈ 7 to t ≈ 10 fm/c) seems to produce some (limited) amount of entropy : about half a unit per baryon. This obviously comes to collisions, which act as a source of viscosity.

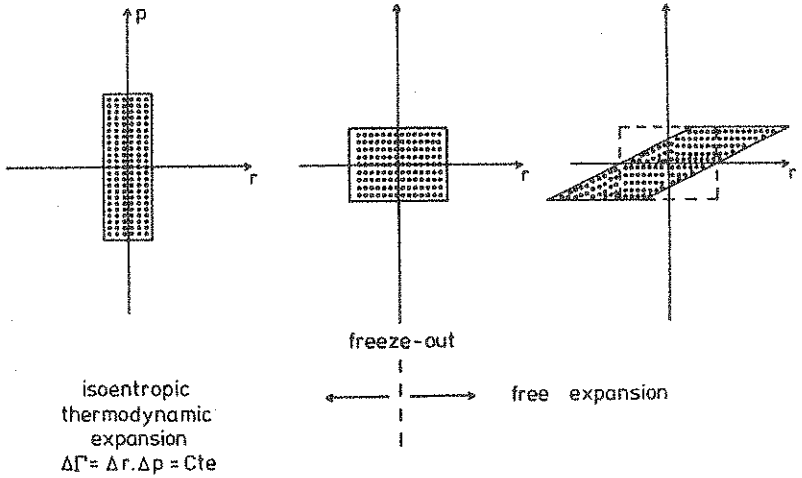

Fig. 13. Schematic illustration of the freeze-out transition showing the building of $\vec{r}.\vec{p}$ correlations.

Recently,[51] it has been shown that such an amount of entropy can be generated by a viscosity of a free nucleon gas. In summary, it seems that the concept of freeze-out is consistent with the cascade dynamics, although some $\vec{r}.\vec{p}$ correlations are built prior to the moment at which NN collisions cease.

5. HYDRODYNAMICS

The conservation equations obtained from the Landau kinetic equation (3.18) (we however drop here the (1 - $\tilde{f}$) factors) are Eqs. (3.27), (3.32) and (3.39). They however imply unknown quantitie and are not closed on themselves. The usual way to close them is phenomenological. The starting point is to observe that the collisic term vanishes for

$$f_1(\vec{r},\vec{p},t) = \rho(\vec{r},t)(2\pi m T)^{-3/2} \exp\left(-\frac{(\vec{p} - m\,\vec{u}(\vec{r},t))^2}{2m\,T}\right) \quad , \tag{5.1}$$

which corresponds to a local equilibrium. The Boltzmann constant is set equal to one. In this case,

$$S_{ij} = \frac{1}{3}\,p\,\delta_{ij} \quad , \quad p = \rho\,T \quad , \quad \vec{J} = 0 \quad . \tag{5.2}$$

In general, (5.1) does not provide a stationary solution, even if we remove the t-dependence. The reason is that the convection term in the l.h.s. of the Landau equation drives particles from one point to the other. Obviously, corrections to (5.1) will come from gradients of the intensive macroscopic quantities ρ , $\vec{u}$ and T. Because S is a second rank tensor, it should be corrected as

$$S_{ij} = \frac{1}{3} p\, \delta_{ij} - \eta(\nabla_j u_i + \nabla_i u_j - \frac{2}{3} \delta_{ij} \vec{\nabla}.\vec{u}) - \zeta\, \delta_{ij} \vec{\nabla}.\vec{u} \quad (5.3)$$

where η and ζ are the shear and bulk viscosity coefficients, respectively. Similarly, the heat flow should be of the form

$$\vec{J} = - \lambda \vec{\nabla} \rho - \varkappa \vec{\nabla} T \quad , \quad (5.4)$$

where $\varkappa$ is the thermal conductivity. Therefore, the basic equations are the continuity equation (3.27), Eq. (3.32) with S_{ij} given by (5.3) and the energy equation (3.39) with the expressions (5.3) and (5.4). They are known as the Navier-Stokes equations describing the behaviour of a real fluid. They still contain too many unknowns. The situation is cured by eliminating the pressure and the internal energy in terms of ρ and T. The functional relationship is assumed to be the same as in equilibrium and is known as the equation of state

$$p = p(\rho,T) \quad (5.4a)$$

$$e = e(\rho,T) \quad . \quad (5.4b)$$

One thus ends with five scalar equations for five variables $(\rho,\vec{u},T)$.

It should be realized that the hydrodynamical approach *basically* assumes a local equilibrium. In other words, it averages over all the local fluctuations inherent to the microscopic structure of the system. In particular, all the fluctuations with characteristic length smaller than the thermalization mean free path λ_{th} are averaged out. In principle, hydrodynamics can describe disturbances with a scale not smaller than λ_{th}. The latter quantity is not necessarily the usual mean free path λ, because in a collision, a particle can lose a very small amount of energy. This is precisely the case in the GeV/A range, where a particle needs at least two or three collisions to be thermalized.[52,53] The quantity λ_{th} is certainly not small compared to the dimension of the system and hydrodynamics is hardly expected to be valid. On the other hand, just to close the discussion about hydrodynamics in general, it should be mentioned that this approach is not necessarily restricted to weakly interacting gases. Actually, the Euler equation (i.e. the Navier-Stokes without viscosity) may be derived in very general grounds, once one has decided to forget about microscopic fluctuations.

Even though, hydrodynamics has been applied very soon in this field because one is dealing with supersonic velocities. Actually, the hydrodynamical equations admit shock wave solutions (due to their non-linearity). The shock compression and heating are linked (for a plane shock) by the Rankine-Hugoniot equation, (that we write here in its relativistic form)

$$(e^2 - e_o^2) + p(\frac{e}{\rho} - \frac{e_o}{\rho_o}) = 0 \quad (5.5)$$

In this equation, which applies to the rest frame of the compressed matter, the indexed quantities correspond to the before-shock zone. The interesting feature of this equation is that one can study the collision between identical nuclei, if we idealize them as two slabs (infinite in the perpendicular direction). The after shock energy density e must be equal to the initial energy density as seen in the c.m. frame :

$$e = \gamma_{c.m.}\, e_o \quad , \quad (5.6)$$

with

$$\gamma_{c.m.} = (1 + \frac{T_{lab}}{2W_o})^{\frac{1}{2}} \quad , \quad W_o = m_N c^2 - B \quad , \quad (5.7)$$

T_{lab} being the lab incident kinetic energy. For a given equation of state $e = e(\rho,s)$, (s = entropy density), Eqs. (5.5) and (5.6) can yield a solution for ρ, s and p for any energy T_{lab}. In particular, if we take an ideal gas ($e = \frac{3}{2}\, p\, \rho^{-1}$), one readily obtains

$$\frac{\rho}{\rho_o} = \frac{5}{2} (\gamma_{c.m.}(E) - \frac{3}{2} \gamma_{c.m.}^{-1}(E)) \quad . \quad (5.8)$$

It has been shown that shocks can generate high entropy (S/A $\approx$ 1-4), high compressions ($\rho/\rho_o \approx$ 2-6) and high temperatures.[56]

Solving the Navier-Stokes equations in three dimensions is a formidable task and has not been carried out up to now. But solving the Euler equations is feasible and has been done. Numerical cell-size effects introduce the so-called "numerical" viscosity,[48,57] whose control is not complete and which seems to be small.[58]

Since one is measuring particles, the microscopic structure has to be reintroduced at some place making comparison with data possible. This is generally done by assuming the fluid cells "freeze out" when the density comes below a certain value ρ_f. The most sophisticated method is to determine the yield and the spectra of different particles by a chemical equilibrium calculation using

the parameters of the cells : ρ_f, T and its flow velocity. The cross-sections for a specific species seem to be sensitive to the freeze-out procedure,[59,60] but the sum charge cross-sections are roughly insensitive.

Figure 14 illustrates the results of an hydrodynamical calculation[62] when the transport coefficients are set equal to zero.

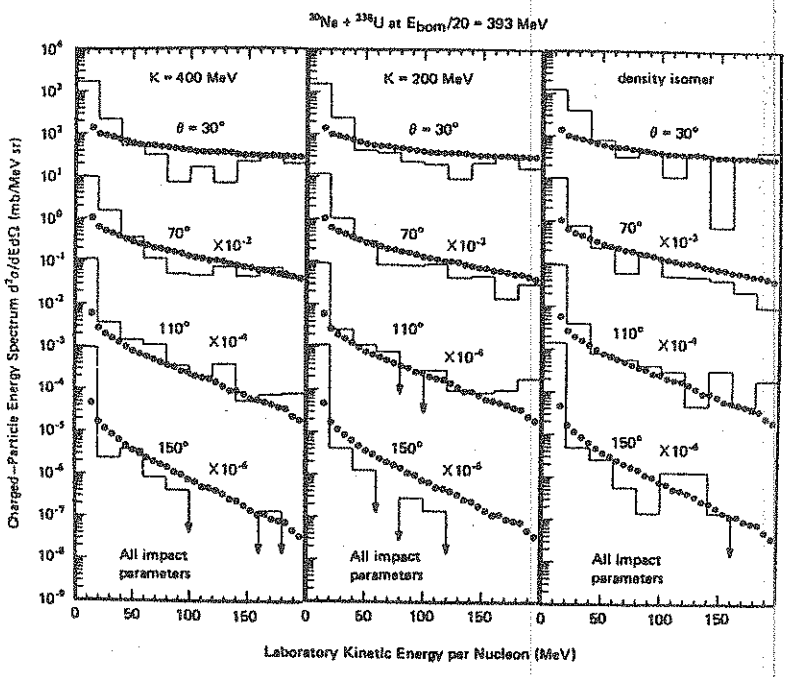

Fig. 14. Comparison of charge-inclusive data[61] (dots) with nonviscous hydrodynamical calculations[62] (histogram). Results for three equations of state are shown.

The results are good on the qualitative level only. Figure 14 touches also at the sensitivity of the results on the equation of state. Due to the large uncertainty of the calculation, it is hard to tell anything about a possible sensitivity. Recent calculations[63] seem to indicate that some observables like the flow angle is sensitive to detail of the equations of state (see later).

So far, the full Navier-Stokes equation could be solved only in the two-dimensional approximation.[60,64,65] The viscosity effects make the entropy increase by only ≈ 20 %.

Definite evidence for the validity of hydrodynamics or even for the manifestation of some specific features has not yet been obtained. Two candidates for such an evidence are the sidewards proton emission in Ne + U at 400 MeV/A[66] and the recent Nb + Nb data at 400 MeV/A.[65] We will discuss these two points in the next section.

6. TOWARD HOT DENSE MATTER PHYSICS ?

6.1. Introduction

As said in the introduction, the difficult task is to relate observables to the properties of the intermediate excited, compresse system, and hopefully to connect these ones to bulk properties of nuclear matter. The inclusive measurements are not very useful in th respect as they are largely dominated by phase space (more exactly, the volume of the available momentum space). In the huge amount of data accumulated, three of them (at least) seem or have seemed promising in this perspective. We are going to discuss them successi vely. The following procedure will be adopted. The INC model, which embodies a trivial equation of state will serve as a reference for "conventional" physics. Hydrodynamics will be looked for indication of eventual equation of state effects.

6.2. Deuteron formation and the entropy puzzle

It is an experimental law[12,67-69] that the production cross-section for a fragment A in the participant region is related to proton cross-section by

$$E_A \frac{d^3\sigma_A}{d p_A^3} = C_A \left(E_p \frac{d^3\sigma_p}{d p^3}\right)^A \quad , \qquad (6.1)$$

where $E_A = A E_p$, $\vec{p}_A = A\vec{p}$, and where C_A is a constant independent of energy and angle. This law at first sight suggested the so-called *coalescence* idea, namely that composite particles are just formed because nucleons can be close to each other in phase space at the end of the collision process. The latter prescription may be made a little bit more precise for the deuteron case in the following equations

$$E \frac{d^3\sigma}{d P^3} = E \int 2\pi b\, d b \int d^3 R\, f_d^{(b)}(\vec{R},\vec{P}) \qquad (6.2)$$

with

$$f_d(\vec{R},\vec{p}) = \frac{3}{4}\int d^3r\, d^3p\, f_2^{np}(\vec{R}+\frac{\vec{r}}{2}, \vec{R}-\frac{\vec{r}}{2}, \frac{\vec{p}}{2}+\vec{p}, \frac{\vec{p}}{2}-\vec{p}) g_d(\vec{r},\vec{p}) \quad , \qquad (6.3)$$

where we have left out the indice b. In the latter equation, f_2^{np} is the two-body distribution function specialized to neutron-proton pairs and $g_d(\vec{r},\vec{p})$ is the distribution function of the relative distance and momentum in the deuteron, normalized to unity. It should be stressed[70-72] that Eq. (6.3) expresses the building of correlations like in a deuteron but does not necessarily exclude that they are carried by heavier composites. The asymptotic emission

of definite composite particle requires knowledge of higher order distribution functions. Therefore (6.2-3) give the cross-section for the formation of ("d") deuteron-like objects. Assuming that the n-p correlations are roughly the same in any light composite, it can be estimated how many "d"'s are present in ^{3}H, ^{3}He,... nuclei. For instance, counting clusters up to ^{4}He, one has

$$\sigma_{"d"} = \sigma_d + \frac{3}{2}(\sigma_{^3H} + \sigma_{^3He}) + 3\,\sigma_{^4He} \quad . \tag{6.4}$$

Similarly, one may define proton-like objects "p" :

$$\sigma_{"p"} = \sigma_p + \sigma_d + \sigma_{^3H} + 2(\sigma_{^3He} + \sigma_{^4He}) + \ldots \quad , \tag{6.5}$$

which is nothing but the charge production cross-section. Formula (6.2-3) are a generalization of the old coalescence model.[67-73] Indeed, if g_d is very sharply peaked in phase space and if $f_2 \approx f_1 f_1$, one readily recovers the power law (6.1) for deuteron emission. The coefficient C_A may even be computed if one takes a gaussian form for g_d

$$g_d(\vec{r},\vec{p}) = \frac{1}{(r_o\sqrt{\pi})^3}\,\frac{1}{(p_o\sqrt{\pi})^3}\,\exp\left(-\left(\frac{r}{r_o}\right)^2 - \left(\frac{p}{p_o}\right)^2\right) \quad , \tag{6.6}$$

and for f_1 (j = n,p)

$$f_1^{(j)}(r,p) = \frac{N_j}{(R_o\sqrt{\pi})^3}\,e^{-\frac{r^2}{R_o^2}}\,\frac{1}{(\sqrt{2\pi\, m\, T})^3}\,e^{-\frac{p^2}{2\,m\,T}} \tag{6.7}$$

where N_j is either the neutron or proton number. In this case, one gets

$$f_d(\vec{R},\vec{P}) = \frac{3}{4}\,\frac{1}{\left(1+\frac{r_o^2}{2R_o^2}\right)^{3/2}\left(1+\frac{p_o^2}{m\,T}\right)^{3/2}}\,f_1^{(n)}\left(\vec{R},\frac{\vec{P}}{2}\right)\,f_1^{(p)}\left(\vec{R},\frac{\vec{P}}{2}\right) \tag{6.8}$$

If one assumes that only N_j is b-dependent in (6.7), one readily gets (for N = Z systems)

$$\left(\frac{d^3\sigma}{d\,P^3}\right)_d = C_d\left[\left(\frac{d^3\sigma_p}{d\,p^3}\right)_{p=\frac{P}{2}}\right]^2 \quad , \tag{6.9a}$$

with

$$C_d = 48 \times \frac{1}{\sigma_o}\,\frac{\hbar^3}{(\sqrt{2\pi}\,R_o)^3}\,\frac{1}{\left(1+\frac{r_o^2}{2R_o^2}\right)^{3/2}\left(1+\frac{p_o^2}{mT}\right)^{3/2}} \quad , \tag{6.9b}$$

and

$$\frac{1}{\sigma_o} = \frac{\int 2\,\pi\,b\,d\,b\,N_p^2(b)}{\left(\int 2\,\pi\,b\,d\,b\,N_p(b)\right)^2} \approx \frac{3}{8}\,\frac{1}{\pi\,b_{max}^2} \quad . \tag{6.9c}$$

The above argumentation leads to a power law between deuteron-like and proton-like cross-sections, whereas the experimental law (6.1) holds for free particles. Whether this difference is meaningful or not has never been investigated. The correction term in r_o/R_o was introduced for the first time in Ref. 74. In general, r_o is small compared to R_o and Eq. (6.9b) reduces to

$$C_d \approx \frac{48}{\sigma_o}\,\frac{1}{(\sqrt{2\pi}\,R_o)^3}\,\frac{1}{\left(1+\frac{p_o^2}{mT}\right)^{3/2}} \quad . \tag{6.9d}$$

The coefficient $p_o \approx 200$ MeV/c ($\approx \hbar/r_o$ because of the normalization of g_d) and therefore the temperature dependence (which reflects the bombarding energy dependence) is not likely to be observed. In passing, we notice that the same calculation can be carried out if there is some $\vec{r}.\vec{p}$ correlations, like $(-1 \leq y \leq 1)$

$$f_1(\vec{r},\vec{p}) \sim e^{-\frac{r^2}{R_o^2}}\,e^{-\frac{p^2}{2mT}}\,e^{-2y\,\frac{\vec{r}.\vec{p}}{R_1\sqrt{2mT}}} \quad . \tag{6.10a}$$

In this case, the r.h.s. of Eq. (6.9b) must be multiplied by

$$(1+y^2)^{-3}\left(1+y^2\,\frac{r_o^2}{(r_o^2+2\,R_o^2)}\,\frac{p_o^2}{p_o^2+mT}\right) \quad . \tag{6.10b}$$

In view of the uncertainty on the parameters entering in (6.9b) and (6.10b), it is hardly believable that one can extract the value of y from experiment, but the analysis has never been undertaken.

A very puzzling aspect of the deuteron production is that a

thermal model[83] (see also refs. 84-87) can also reproduce the power law (6.1). Such a model yields

$$\frac{N_d}{N_n N_p} = \frac{3}{4V} \exp(B/T) \quad , \tag{6.11}$$

where V is the volume of the thermalized system and B is the deuteron binding energy. For the heavy ion case, the argument of the exponential is very small. One has an expression similar to (6.9a) with this time

$$C_d = \frac{48}{\sigma_o} \frac{1}{\sqrt{2}} \frac{\hbar^3}{V} \quad , \tag{6.12}$$

which as we said is very similar to (6.9c). Thus the power law may come from two very different dynamical schemes. Either the deuterons are formed by chance at the freeze-out or they are regularly created and destroyed during the collision process. Let us however mention that the deuteron cross-section has been calculated by Eqs. (6.2)-(6.3) using the INC model to evaluate the two-body distribution function, in Refs. 70,74. The results of Ref. 74 are presented in Fig. 15.

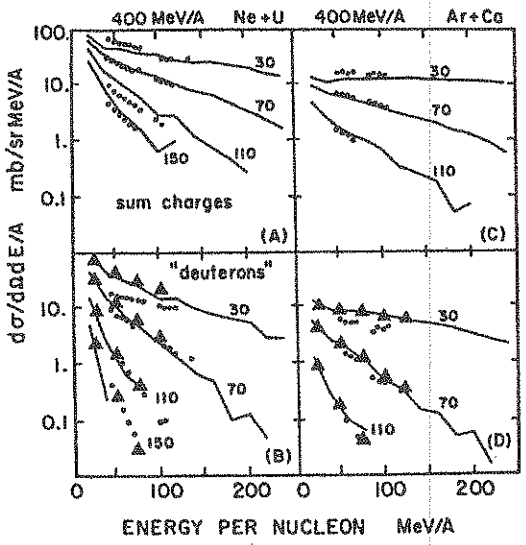

Fig. 15. Comparison between the INC calculation of Ref. 74 and the proton-like and deuteron-like (triangles) experimental cross-section. For the deuterons, the dots indicate the free deuteron yield. The experimental data are from Ref. 75.

their last interaction. The agreement is within a factor 2, which is remarkably good. The latter result is quite interesting from another point of view, since it may explain the peak at non-zero angle in the proton cross-section (see Section 5). Actually the sum charge (primordial proton) cross-section would be maximum at 0^o, but in this region, the nucleons would be so numerous that they would be "eaten up" by the deuteron formation. For more detail, see Ref. 4.

The fact that coalescence and thermal models give similar results may be accidental or due to the deuteron formation mode in a thermal model. Indeed, in a kinetic model (applicable to dilute gases), the deuteron balance would be given by (we forget the convection term)

$$\frac{\partial}{\partial t} f_d(\vec{P}_{23}) = \int d^3p_1\, d^3p_2\, d^3p_3\, d^3p_1' \{f_1(\vec{p}_1)\, f_1(\vec{p}_2)\, f_1(\vec{p}_3)\, f_1(\vec{p}_1') W(\vec{p}_1,\vec{p}_2,\vec{p}_3 \to \vec{p}_1', \vec{P}_{23}) - f_1(\vec{p}_1')\, f_d(\vec{P}_{23})\, W(\vec{p}_1', \vec{P}_{23} \to \vec{p}_1\vec{p}_2\vec{p}_3)\} \quad , \tag{6.13}$$

since the energy-momentum conservation requires a third partner (n+p+N → N+d). However, because the deuteron is almost unbound, the transition probability is close to

$$W(\vec{p}_1,\vec{p}_2,\vec{p}_3 \to \vec{p}_1',\vec{p}_{23}) \approx \delta(\vec{p}_1-\vec{p}_1')\, \delta(\vec{p}_2+\vec{p}_3-\vec{P}_{23})\, w(\vec{p}_2,\vec{p}_3,\vec{P}_{23}) \quad . \tag{6.14}$$

If the dynamics is such that the nucleons close in phase space inevitably makes a deuteron, one may write

$$W(\vec{p}_1,\vec{p}_2,\vec{p}_3 \to \vec{p}_1',\vec{P}_{23}) \approx \delta(\vec{p}_1-\vec{p}_1')\, \delta(\vec{p}_2-\frac{\vec{P}_{23}}{2})\, \delta(\vec{p}_3-\frac{\vec{P}_{23}}{2}) \tag{6.15}$$

Therefore

$$\frac{\partial}{\partial t} f_d \propto f_1(\frac{\vec{P}_{23}}{2})\, f_1(\frac{\vec{P}_{23}}{2}) - f_d(P_{23}) \quad . \tag{6.16}$$

The equilibrium condition requires

$$f_d(\vec{P}) \approx f_1(\frac{\vec{P}}{2})\, f_1(\frac{\vec{P}}{2}) \quad , \tag{6.17}$$

which is the basic coalescence relation.

Whatever the deuteron source is, there is a relationship between the deuteron yield and the entropy gained by the system. Originally, this has been established by Siemens and Kapusta[76] using the thermal model. The same relation can be derived on the basis of relation (6.3). We follow the presentation of Ref. 70. The number of deuteron-like particles is given by

$$N_{"d"} = \frac{3}{4} \int d^3R\, d^3P \int d^3r\, d^3p\, f_2^{np}(\vec{R}+\frac{\vec{r}}{2}, \vec{R}-\frac{\vec{r}}{2}, \frac{\vec{P}}{2}+\vec{p}, \frac{\vec{P}}{2}-\vec{p})\, g_d(\vec{r},\vec{p}) \quad . \tag{6.18}$$

If we assume g_d to be very narrow and $f_2 \approx f_1 f_1$, we obtain (for a N = Z) system

$$N_{"d"} = \frac{3}{16} \int d^3R\, d^3P\, [f_1(\vec{R},\frac{\vec{P}}{2})]^2 \quad , \tag{6.19}$$

where f_1 refers to nucleon, either proton or neutron. We may write (6.19) as

$$N_{"d"} = \frac{3}{2} \langle f_1 \rangle \int d^3r\, d^3p\, f_1(\vec{r},\vec{p}) = \frac{3}{2} \langle f_1 \rangle N_{"p"} \quad . \tag{6.20}$$

In this equation $\langle f_1 \rangle$ is the average of f_1 on its own distribution

$$\langle f_1 \rangle = \frac{\int d^3r\, d^3p\, [f_1(\vec{r},\vec{p})]^2}{\int d^3r\, d^3p\, f_1(\vec{r},\vec{p})} \quad . \tag{6.21}$$

Now, the entropy (Eq. (4.8)) is given by

$$\frac{S}{A} = 1 + 4\, \ell n\, 2 - \langle \ell n\, f_1 \rangle \quad . \tag{6.22}$$

By the Sackur-Tetrode formula, one may relate $\langle \ell n\, f_1 \rangle$ to $\ell n\, \langle f_1 \rangle$. Using numerical values, one gets

$$\frac{S}{A} = 3.95 - \ell n \frac{N_{"d"}}{N_{"p"}} \quad . \tag{6.23}$$

In Ref. 76, the same relation is obtained, but, since the dilute gas limit is used, the formula involves free deuterons and protons. The physical content of Eq. (6.23) is rather transparent. The larger the entropy is, the farther from each other the nucleons are in phase space, the smaller the chance of building deuterons is.

Originally, the entropy was extracted (through (6.23)) from *integrated* deuteron cross-section and compared to ordinary equation of state and to INC evaluations (Eq. (4.8)) for central collisions. The "experimental" entropy was found substantially larger than the theoretical estimates, as shown in Fig. 16. The full curve is a one-dimensional hydrodynamical calculation with two adjusted parameters (η and ρ_f , see Section 5). It contains however an interesting aspect. At low incident energy, few entropy is created and many heavy clusters are expectedly formed. At the freeze-out, many of them decay into smaller ones increasing the observed deuteron yield. Apart from this aspect, which is effective at low energy only, there is a large discrepancy between theory and experiment : this constitutes the so-called *entropy puzzle*. There has been several propositions to remove the puzzle, like the excitation of new degrees of freedom[76] or the reduction of the deuteron binding force inside a medium,[78] a very similar effect to the Mott transition in a plasma.

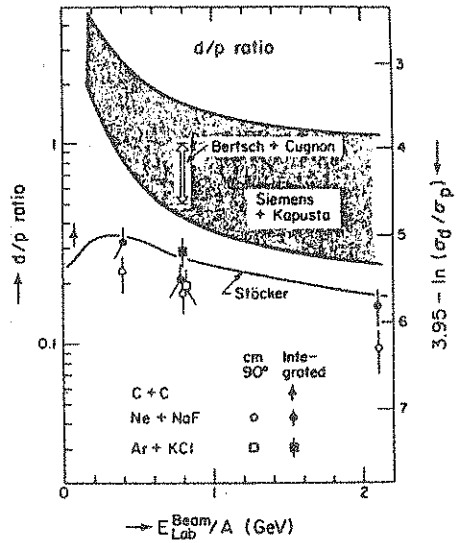

Fig. 16. Observed d/p ratios and entropy. Data for equal-mass collisions are compared with various theoretical predictions by Siemens and Kapusta (thermal),[76] Bertsch and Cugnon (cascade),[70] and Stöcker (hydrodynamics + thermal break-up).[77] Adapted from Ref. 12.

The explanation comes very likely from a strong impact parameter or multiplicity dependence. The charged multiplicity dependence of the "d"/"p" ratio has been demonstrated by Gutbrod's group[80] and later by Nagamiya's group.[81] Their results are contained in Fig. 17, along with INC calculations for Ar + KCl.[23,50,82] Interestingly enough, the "d"/"p" increases with the charge multiplicity (both experimentally and theoretically), suggesting that the occupation in phase space is substantially larger in high multiplicity (central) collisions. The question which naturally arises is whether a saturation really occurs and why it occurs. According to Refs. 23, 70, 82, the bulk dynamics can occur for small impact parameters only, because particles which are within a mean free path from the surface do not participate to the phase space spreading in the same way, even if in the momentum space, there is perhaps no real difference. They are not confined by outer parts of the system. The situation is illustrated in Fig. 18, which shows a steady decrease of the calculated entropy as b decreases leading to a sort of saturation for small impact parameters. The content of Fig. 19 goes in the same direction showing that relation (6.23) holds quite well for small impact parameters. For all these reasons, it is more reasonable to compare saturation (or maximum) values of Fig. 17 with theory (if the latter cannot predict surface effects), rather than integrated quantities, like in Fig. 16.

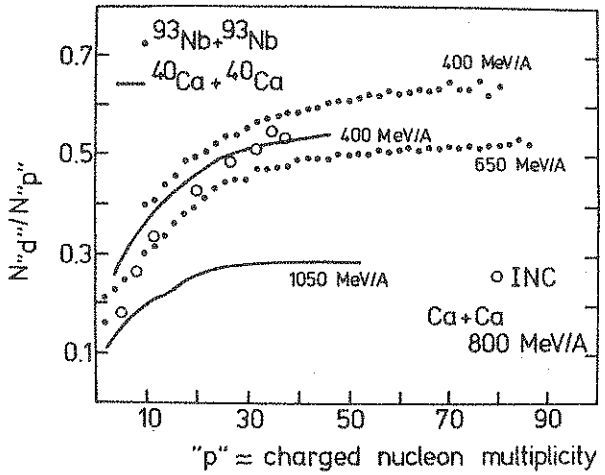

Fig. 17. Experimental "d"/"p" ratio versus charged multiplicity for four systems. The full dots are data from Ref. 81, the lines represent the data of Ref. 80 and the open dots are calculations from Ref. 82. For the latter the abscissa represents half the average participant number for several impact parameters ranging from zero to 7.15 fm.

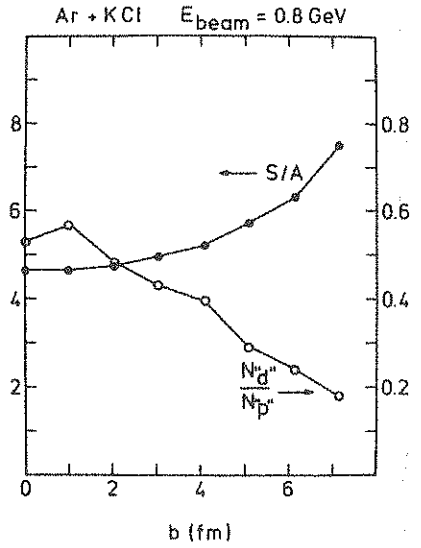

Fig. 18. INC calculation of the entropy per baryon and the deuteron proton ratio as a function of impact parameter. Adapted from Ref. 82

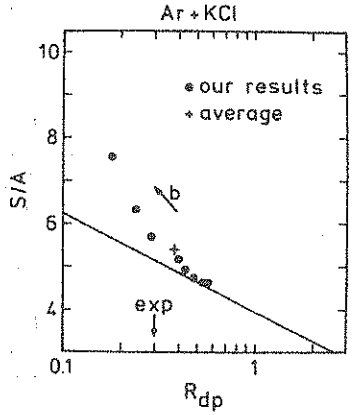

Fig. 19. INC calculated entropy and "d" over "p" ratio compared with Eq. (6.23) (full line). The dots correspond to regularly spaced impact parameters ranging from 0 to about 7.5 fm. The arrows indicate the experimental value of $R_{dp} = N_{"d"}/N_{"p"}$ when integrated cross-sections are used. Adapted from Ref.82

One then obtains Fig. 20, where the experimental bulk entropy is somewhat between 4 and 5 units, whereas the INC model predicts a value a little too small. The original "puzzle" has thus substantially deflated, but the remaining discrepancy should not be underestimated, since it corresponds to a phase space occupancy, wrong by ~ 40 %.

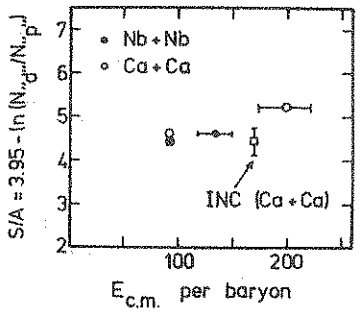

Fig. 20. Experimental values of the "d"/"p" ratio (or the entropy) for large multiplicities compared to the INC calculations of Ref. 70.

6.3. Pion multiplicity and compression energy

A very important piece of data was obtained by the Stock's streamer chamber group[88] and is shown in Fig. 21.

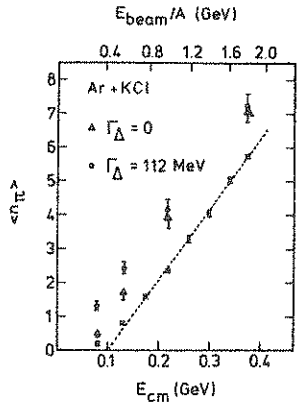

Fig. 21. The negative pion yield measured by a central trigger for Ar + KCl collisions (data around the dotted line) is compared to the prediction of INC (circles). The triangles are the results obtained in a calculation with frozen Δ-isobars. Taken from Ref. 14.

Here is presented the (negative) pion multiplicity from the central trigger, which, according to Ref. 88, collects all the small impact parameters up to b = 2.2 fm. To understand fully the importance of these data, it is useful to remind of two complementary experimental results. (1) The pion multiplicity distribution is consistent with incoherent production,[88,89] which, for a given impact parameter, implies a Poisson law.[90] (2) There is a strong correlation between the pion and the charge multiplicity,[88,89] heavily suggesting that central collisions produce most of the pions. Figure 21 has been the starting point of a long-standing debate. The INC calculations of Ref. 14, which was the most reliable calculation at that time, was not able to reproduce the data. If the following reactions were considered

$$NN \rightleftarrows N\Delta \quad , \quad N\Delta \rightarrow N\Delta \quad , \quad \Delta\Delta \rightarrow \Delta\Delta \qquad (6.24a)$$

with pions coming from the decay of the Δ's at the end of the cascade, the multiplicities (triangles in Fig. 21) came out rather well, but the spectrum was really bad (see Ref. 14 for the detail). If the following reactions

$$\Delta \rightleftarrows \pi N \qquad (6.24b)$$

were introduced during the cascade, on the basis of the natural Δ lifetime, the spectrum is very much improved, but the pion multiplicity is overestimated (circles in Fig. 21), especially close to the effective threshold. The increase of the pion yield simply reflects the higher energy which is required to make a pion if only (6.24a) is retained, because of the large mass of the Δ-resonance.

The discrepancy between INC predictions (with (6.24b)) and experiment has been interpreted by the authors of Ref. 91 as a manifestation of the compression energy. The idea is the following. A part of the available energy is necessary to compress the matter and therefore less kinetic energy is available to produce pions. This demands two subsidiary conditions. First, the number of pions is just determined by the kinetic (or thermal) energy. Second, the number of pions is fixed at (or by) the maximum density. The latter observation is corroborated by the INC calculation of Ref. 13,14. At the maximum compression, there are almost only Δ particles. During the expansion, the number of Δ's diminishes, but the number of free pions is compensating this decrease. Globally, the total number of pions (free + those hidden in Δ's) seems to stay constant after the moment of maximum compression. Therefore, it seems that one may write

$$n_\pi^{INC}(E_o) = f^{INC}(E_o, \bar{\rho}) \quad , \qquad (6.25)$$

which expresses that, within the frame of the INC model, the number of pions is a function (whose analytical form is unknown) of the initial energy (which is the same as the kinetic energy) and of the average maximum density $\bar{\rho}$. In Ref. 91, it is assumed that, in the real world, the function is the *same* as in (6.25), but that the available energy is reduced by the compression energy :

$$n_\pi^{exp}(E_o) = f^{INC}(E_o - E^c(\bar{\rho}), \bar{\rho}) \quad . \qquad (6.26)$$

Comparison between (6.25) and (6.26) is then used to extract $E^c(\bar{\rho})$, when $\bar{\rho}$ is taken from the INC evaluation. The results are given in Fig. 22, and are remarkable in several respects. Let us just mention that the compression energy is obtained for a wide range of densities The procedure of Ref. 91 has been very much disputed, because it looks like taking some good aspects from a model and rejecting some bad aspects at the same time. However, it is fair to say that the authors of Ref. 91 have been very careful to eliminate all subsidiary sources of uncertainty, as by making an independent analysis in terms of multiplicity rather than in energy. Moreover, Harris and Stock[92] have made a similar analysis, abandonning the hypothesis (6.25) in favour of

$$n_\pi^{exp}(E_o) = f^{th}(E_o - E^c(\bar{\rho}), \bar{\rho}) \quad , \qquad (6.27)$$

i.e. using a thermal model. The only reference to the INC model is the value of $\bar{\rho}$, which is borrowed from it. They arrived at the same

result. (Incidentally, it means that chemical equilibrium is more or less realized in the INC). This additional result makes the analysis more convincing, but the whole procedure leaves still some skepticism. Nevertheless, it seems that the discrepancy is so large at small energy that something should be lacking in the INC model.

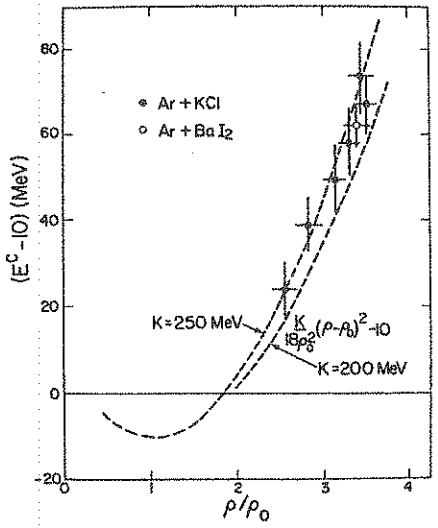

Fig. 22. Compression energy versus the density as determined from the comparison between Eqs. (6.25)-(6.26). See text for detail. Taken from Ref. 91.

Let us remind that the basic premise of the INC is the assumption that the collision process is a sequence of binary collisions between on-shell particles proceeding as in free space. If the model fails somewhere, either the whole model should be rejected (this would be unlikely in view of the numerous successes of the model) or one (or several) of the assumptions (indicated by the underlined terms) have to be relaxed. For the last choice, one may think of several possibilities. Most of them have concentrated on the second assumption. In most cases, the idea is to introduce in one way or the other an average potential for the nucleons.

In Ref. 93, the particles are put off their mass shell to simulate the initial binding effects and they are allowed to come on their mass shell once they make a collision. This procedure is inspired by the observation that particles are spreading very fast in phase space. Presumably, the average field is destroyed at the same rate.

In Ref. 94, the standard INC model is run to calculate the average density and by a simple folding method the average field. Then the cascade is run again with an average field (a model close to the Landau equation). In Ref. 95, the influence of a hard core is added through the Enskog procedure.[96,97] Let also mention that the effect of interaction on the pion multiplicity has also been studied recently[30] in a kind of equation of motion approach. All these approaches aimed to introduce interaction energy effect. It is not clear however whether an average potential, a one-body property, can account for the interaction energy, a two-body property. In addition, one is facing in all these approaches a "double-counting" problem. If a part of the dynamics is put into an average field, the free collision term should be corrected for that. We will not discuss this topic any further, because the situation is far from clear for the time being.

Let us finally notice that the relaxation of the third assumption has not been investigated up to now. One may very well conceive that the production mechanism of the pions is very much altered by the presence of the surrounding matter. Also, nobody has looked at the influence of the pion propagation.

In conclusion, it is very likely that interaction energy effects are manifestating themselves in the excitation function of the pion multiplicity, but one is still far from extracting the function $E^c(\rho)$ without any ambiguity.

6.4. Collective flow

One usually characterizes as collective a phenomenon by which several particles behave cooperatively to the construction of a physical quantity. Expectedly, a collective behaviour arises from the bulk properties of the system (although nuclear physics has accustomed us with collective vibrations which involve single-particle properties coupled to surface degrees of freedom). At least, there exists a good example : the giant isoscalar monopole state. Its energy is given (asymptotically, i.e. as $A^{-1} \to 0$) by the compression modulus of nuclear matter.

A collective flow would thus correspond to a correlated emission of particles (or momentum or energy) in a preferential direction. The hydrodynamics basically relying on the bulk properties of matter, it was originally believed that the observation of a collective flow would provide an evidence of hydrodynamical behaviour. Now, it seems to us that the issue can be formulated in two questions : (1) How to put in evidence a collective flow ? (2) Are there different predictions of the flow in the frame of INC and hydrodynamics, respectively ?

In the relativistic heavy ion case, we have already indicated that signals of a collective flow are possibly given by the proton angular distribution in Ne + U at 400 MeV/A [59] and by the comparison between proton and pion temperatures, which could indicate an explosive radial expansion.[15] But it is generally believed that the

collective flow will be brought to light more easily by studying the so-called global variables.[98-105] They have been used successfully in high-energy physics to put jets in evidence in high multiplicity events. The idea is to characterize with a few numbers the topology of an event with a large number of ejectiles, whose exact description would require many and many variables. The most common of the global variables is the sphericity tensor

$$Q_{ij} = \sum_{\nu} \gamma(p^{\nu})\ p_i^{\nu}\ p_j^{\nu} \quad , \tag{6.28}$$

where p_i^{ν} is the i^{th} Cartesian coordinate (in the c.m. system) of the momentum of the ν^{th} ejectile. The quantity $\gamma(p^{\nu})$ is a (scalar) weighting factor. The most interesting choices are

$$\gamma = 1/|p^{\nu}| \quad , \quad 1/2m_{\nu} \quad , \quad 1/(p^{\nu})^2 \quad , \tag{6.29}$$

well suited to study the flow of momentum, energy and number of particles, respectively. For $\gamma = 1$, the sphericity tensor is a part of the phase space tensor (4.6), when proper average over events has been carried out. The choice $\gamma = 1/2m_{\nu}$ deserves particular attention, since it is coalescence-invariant. This means that a deuteron has the same weight as two nucleons having the same velocity. Such a choice is very well suited to models which do not include composite formation explicitly.

Geometrically, the tensor (6.28) represents an ellipsoid, which has three axes and three eigenvalues λ_i , $i = 1,2,3$, that we label in decreasing order. We call $\vec{e}_i$ the corresponding normalized eigenvectors. The eigenvalues are given by (this time, not necessarily in descending order)

$$\lambda_i = \frac{1}{3}\ \mathrm{tr}\ \underset{\approx}{Q} + 2p\ \cos\left[\frac{1}{3}\cos^{-1}\left(\frac{r}{p^3}\right) + (n-1)\frac{\pi}{3}\right] \quad , \tag{6.30}$$

with

$$p = \frac{1}{3}\left[(\mathrm{tr}\ \underset{\approx}{Q})^2 - 3\ A\right]^{\frac{1}{2}} \quad , \tag{6.31}$$

$$r = \frac{1}{6}\left(A\ \mathrm{tr}\ \underset{\approx}{Q} + 3\ B\right) + \frac{1}{27}\left(\mathrm{tr}\ \underset{\approx}{Q}\right)^3 \quad , \tag{6.32}$$

$$A = \sum_{\{ij\}} \left(Q_{ii}\ Q_{jj} - Q_{ij}^2\right) \quad , \tag{6.33}$$

$$B = \sum_{[ij\ k]} \varepsilon_{ijk}\ Q_{1i}\ Q_{2j}\ Q_{3k} \quad . \tag{6.34}$$

In Eq. (6.33), the summation extends over the combinations of the three indices two by two. In Eq. (6.34), the summation runs over the permutations and ε_{ijk} is the usual antisymmetric tensor. Since Q_{ij} contains six independent numbers, three additional quantities are needed to complete the description of the ellipsoid, namely to give its orientation. They are usually taken as the polar angles (ϑ,φ) of the largest axis with respect to the x,y,z axes (let us remind that the z-axis coincides with the beam axis), and χ, the third Euler angle (i.e. the angle between the second largest axis and the intersection between the $(\vec{e}_x, \vec{e}_y)$ plane and the $(\vec{e}_2, \vec{e}_3)$ plane. Since the trace of $\underset{\approx}{Q}$ is a conserved quantity (for usual γ's), one of the variables is useless. It is customary to consider the aspect ratios

$$q_1 = \frac{\lambda_1}{\lambda_3} \quad , \quad q_2 = \frac{\lambda_2}{\lambda_3} \quad , \tag{6.35}$$

instead of the three eigenvalues. The physically accessible values of q_1 and q_2 are given in Fig. 23.

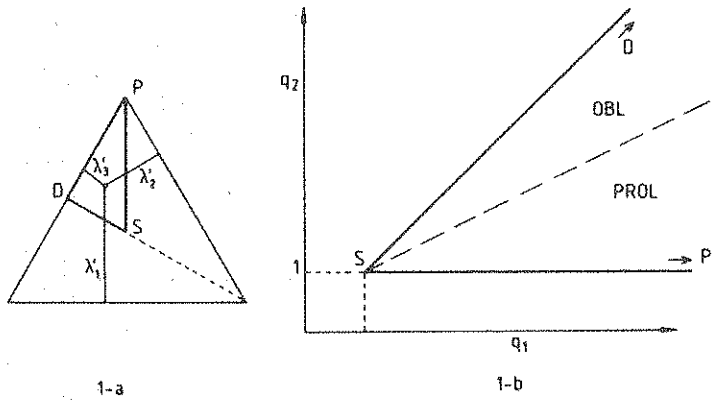

Fig. 23. Two ways of characterizing the shape of an ellipsoid. See text for more detail. The heavy lines delineate the accessible area. P = pencil, S = sphere, D = disk. The primes indicate that the eigenvalues are normalized to $\lambda_1' + \lambda_2' + \lambda_3' = 1$. Adapted from Ref. 102.

It would be desirable, for the sake of convenience, to characterize events with the smallest possible number of global variables. Generally, one restricts oneself to one shape variable q_1 and one angular variable ϑ. Several other shape variables may be constructed with the eigenvalues λ_i, such as the sphericity

$$S = \frac{3}{2}\ \frac{\lambda_2 + \lambda_3}{\lambda_1 + \lambda_2 + \lambda_3} \quad , \tag{6.36a}$$

the flattness

$$F = \frac{\sqrt{3}}{2} \frac{\lambda_2 - \lambda_3}{\lambda_1 + \lambda_2 + \lambda_3} \quad , \tag{6.36b}$$

the "jettiness"

$$j = \frac{\lambda_1 - \lambda_2}{\lambda_1 + \lambda_2 + \lambda_3} \quad , \tag{6.36c}$$

the "prolateness"

$$\Phi = \frac{\lambda_2 - \lambda_3}{\lambda_1 - \lambda_3} \quad , \tag{6.36d}$$

or the eccentricity

$$\varepsilon = \frac{\lambda_s - \frac{1}{2}(\lambda_2 + \lambda_r)}{\lambda_1 + \lambda_2 + \lambda_3} \quad . \tag{6.36e}$$

In the last relation, λ_s is the eigenvalue for the axis of quasi-symmetry. It is λ_1 if $\lambda_1 - \lambda_2 \geq \lambda_2 - \lambda_3$ and λ_3 if not ; λ_r is the remaining eigenvalue. Another commonly used variable is the thrust, given by

$$T = \max_{\vec{n}} \frac{\sum_\nu |\vec{n}.\vec{p}^\nu|}{\sum_\nu |\vec{p}^\nu|} \quad . \tag{6.37}$$

The direction $\vec{n}_T$ which gives the maximum is the thrust direction. Finally, several simple variables, like the longitudinal energy fraction

$$f_3 = \frac{\sum_\nu (p_3^\nu)^2/2m_\nu}{\sum_\nu (p^\nu)^2/2m_\nu} \quad , \tag{6.38}$$

or the fragment multiplicity N_ν, are considered. The last two variables are simply related to the sphericity tensor :

$$f_3 = \frac{Q_{33}}{\mathrm{tr}\, \underset{\approx}{Q}} \quad , \quad N_\nu = \mathrm{tr}\, \underset{\approx}{Q} \quad , \tag{6.39}$$

for $\gamma = 1/(2m_\nu)$ and $1/(p_\nu^2)$, respectively.

The values of typical shape variables are given in Table 1 for three special types of events : a spherical event, where the emission is isotropic, a disk-like event, where the emission is isotropic in a plane only and a pencil-like event, where particles are emitted in two opposite directions.

Table 1. Values of the global variables for limiting events

Global variable	Sphere	Pencil	Disk
q_1	1	∞	∞
q_2	1	undefined	∞
S	1	0	$\frac{3}{4}$
F	0	0	$\sqrt{3}/4$
j	0	1	0
Φ	undefined	0	1
ε	0	1	$-\frac{1}{2}$
T	$\frac{1}{2}$	1	$2/\pi$

The analysis is made event by event. It is worthwhile to discuss what is actually implied by this procedure. The probability for producting an event with sphericity tensor elements Q_{ij} of value T_{ij} is given by

$$\Phi(T_{ij}) = \sum_N P_N \int d^3p_1 \ldots d^3p_N \; f_N(\vec{p}_1,\ldots,\vec{p}_N) \; \delta(Q_{ij}(\vec{p}_1,\ldots,\vec{p}_N) - T_{ij}) \tag{6.40}$$

where Q_{ij} is the expression (6.28), f_N is the N-body distribution function (in momentum space) and P_N is the probability of having an event with N ejectiles. The average value of Q_{ij} is

$$\langle Q_{ij} \rangle = \int \Phi(T_{ij}) \; T_{ij} \; d\, T_{ij} = \sum_N P_N \int d^3p_1 \ldots d^3p_N \; f_N(\vec{p}_1,\ldots,\vec{p}_N) \; Q_{ij}(\vec{p}_1,\ldots,\vec{p}_N) \quad . \tag{6.41}$$

If the correlations are unimportant ($f_N \approx \prod_i f_1$), this expression reduces to

$$\langle Q_{ij} \rangle = \sum_N P_N \int d^3p\ \gamma(p)\ p_i\ p_j\ f_1\ (\vec{p}) \quad . \tag{6.42}$$

In this case, there is no other information in Q_{ij} than in f_1. (Let us notice that this is not necessarily the same for the λ_i's, since the relation between the λ_i's and the Q_{ij}'s is not linear). The fluctuation of the elements Q_{ij} is given by

$$\sigma^2_{ij} = \langle Q^2_{ij} \rangle - \langle Q_{ij} \rangle^2 \quad . \tag{6.43}$$

With the help of (6.40), we have

$$\langle Q^2_{ij} \rangle = \int \Phi(T_{ij})\ T^2_{ij}\ d\ T_{ij} =$$

$$\sum_N P_N \int d^3p_1 \ldots d^3p_N\ f_N(\vec{p}_1,\ldots,\vec{p}_N)\ [Q_{ij}(\vec{p}_2,\ldots,\vec{p}_N)]^2 \quad . \tag{6.44}$$

If the correlations are negligible, we have

$$\langle Q^2_{ij} \rangle = \langle N(N-1) \rangle \left[\int d^3p\ \gamma\ p_i\ p_j\ f_1(\vec{p})\right]^2 + \langle N \rangle \int d^3p\ \gamma^2\ p^2_i\ p^2_j\ f_1 \tag{6.45}$$

where $\langle N \rangle = \sum_N N\ P_N$; consequently, we have

$$\frac{\sigma_{ij}}{\langle Q_{ij} \rangle} = \frac{1}{\sqrt{\langle N \rangle}} \frac{\left\{\int d^3p\ \gamma^2\ p^2_i\ p^2_j\ f_1 - \left[\int d^3p\ \gamma\ p_i\ p_j\ f_1(\vec{p})\right]^2\right\}^{\frac{1}{2}}}{\int d^3p\ \gamma\ p_i\ p_j\ f_1} \quad . \tag{6.46}$$

This important result, surmised in ref. 102, was obtained in Ref. 105. As we have seen, the averages over f_1 are more or less the same for different (symmetric) systems at the same energy per particle. Therefore, if the correlations play no role, the fluctuations would *decrease* with increasing mass. This is noting but that an extension of the properties of a system described by a canonical ensemble.

Fluctuations on the global variables are not so easy to estimate because they imply averages over eigenvalues and similar quantities, which are non linear functions of the elements Q_{ij}. Furthermore, the fluctuations mix with the so-called Jacobian effects in a very intricate manner. To understand what it means, let us take two simple examples.

(1) Let us assume that the dynamics leads in the average to spherical events. But, because of fluctuations, the ellipsoid is sometimes prolate and sometimes oblate. Now, since $q_1 \geq 1$ by definition, it is evident that $\langle q_1 \rangle$ will be larger than unity and that the difference will be larger and larger when the fluctuations are increasing.

(2) Let us consider events with a fixed elongated shape, but with the major axis pointing in the average toward the beam (z) direction, with fluctuations. It is also clear that the average angle ϑ will be different from zero.

Both examples show the bias introduced by the mapping of a manifold (Q_{ij}) into another one ($\lambda_i, \vartheta, \varphi, \chi$) in such a way that an interior point is transformed into a point on an edge. This is particularly clear for the point $q_1 = 1$ (see Fig. 23) and the point $\vartheta = 0$. This may be formalized in the following way. The differential cross-section for making a tensor of elements T_{ij} is

$$\frac{d^6\sigma}{[d\ T_{ij}]} = \int d^2b \sum_N P_b(N) \int d^3p_1 \ldots d^3p_N\ f_N^{(b)}(\vec{p}_1,\ldots,\vec{p}_N) \prod_{i \leq j} \delta(Q_{ij} - T_{ij}) \tag{6.47}$$

where $[d\ T_{ij}]$ stands for the six-dimensional element. If $f_N^{(b)}$ does not depend on the impact parameter b, one has

$$\frac{d^6}{[d\ T_{ij}]} = \sum_N \sigma_N \int d^3p_1 \ldots d^3p_N\ f_N(\vec{p}_1,\ldots,\vec{p}_N) \prod_{i \leq j} \delta(Q_{ij} - T_{ij})$$

$$= \sum_N \sigma_N\ \Phi_N\ (T_{ij}) \quad . \tag{6.48}$$

If we turn to the eigenvalues and angles, we can write

$$\frac{d^6\sigma}{d\lambda_1\ d\lambda_2\ d\lambda_3\ d\vartheta\ d\varphi\ d\chi} = \frac{\partial(T_{ij})}{\partial(\lambda_1,\lambda_2,\lambda_3,\vartheta,\varphi,\chi)} \frac{d^6\sigma}{[d\ T_{ij}]} \quad , \tag{6.49}$$

where we have introduced the Jacobian of the transformation. It is given by[105]

$$\frac{\partial(T_{ij})}{\partial(\lambda_1,\lambda_2,\lambda_3,\vartheta,\varphi,\chi)} = J(\lambda_i)\ \sin\vartheta \quad , \tag{6.50}$$

$$J(\lambda_i) = (\lambda_1 - \lambda_3)(\lambda_1 - \lambda_2)(\lambda_2 - \lambda_3) \quad . \tag{6.51}$$

The two examples above can be easily formulated. One may start with (Eq. (6.48))

$$\Phi_N(T_{ij}) \alpha \exp\left[-\frac{N}{2} \mathrm{tr}\ \underset{\sim}{I}\ \underset{\sim}{I}_{th}^{-1}\right] \quad , \tag{6.52}$$

where T_{th} is the theoretical value matrix. For case (1) $\underset{\sim}{I}_{th}$ is simply the unit matrix. In that case[105]

$$J(\lambda_i) \sin\vartheta\ \Phi_N(T_{ij}) \alpha \exp\left(-\frac{N}{2} \sum_{i=1}^{3} [\lambda_i - (1 - \frac{4}{N}) \ln \lambda_i]\right) \tag{6.53}$$

It can be checked numerically that this distribution (which has a maximum for $\lambda_1 = \lambda_2 = \lambda_3$) leads however to

$$\langle q_1 \rangle \approx 1 + \frac{3}{\sqrt{N}} + \frac{22}{N} \quad . \tag{6.54}$$

Similarly, case (2) corresponds to $\underset{\sim}{I}_{th} = \mathrm{diag}(1,1,r)$, with $r > 1$. Numerically, this case leads to a maximum in the distribution $dN/d\vartheta$ for the observed angle ϑ, which is away from zero degree. The false maximum may be avoided if one looks at the modified distribution

$$\frac{dN}{d\cos\vartheta} = \frac{1}{\sin\vartheta} \frac{dN}{d\vartheta} \quad . \tag{6.55}$$

A maximum for $\vartheta \neq 0$ in such a quantity can be considered as a manifestation of a true oriented flow. A modification similar to (6.55) can be introduced in the dN/dq_1 distribution to remove the distortion due to the Jacobian. See Ref. 105 for details.

What would be the differences between INC and hydrodynamics concerning the global variables ? Figure 24 gives the general trend of the variation of the average angle ϑ (in the sense of the distribution $dN/d\vartheta$) and of the thrust (here the thrust has been preferred to the first aspect ratio q_1) as a function of the impact parameter for a symmetric system. There is a dramatic difference between the predictions of the two models. Hydrodynamics predicts a *true* flow angle (there is no fluctuation in an ordinary hydrodynamic calculation) at 90° for small impact parameter because of the short mean free path assumption which makes the matter opaque. The INC on the other hand, predicts for b = 0 smaller values of ϑ, but this does not correspond to a true flow in this case, but rather as explained above to the fluctuations. This is particularly well illustrated by Fig. 25. It shows the distribution of the projection of the extremity of the unit vector along the major axis on a plane perpendicular to the beam axis. This plot is free of Jacobian effects, at least around the beam axis. Clearly, for central collisions, the ellipsoid points in the average in the beam direction, with large fluctuations.

Hydrodynamics does predict roughly the same pattern for all (symmetric) systems and energies between, say 250 to 1000 MeV/A. If some energy dependence is predicted,[104] the large flow angles, linked to opacity, are always present. In the INC model, the situation is more subtle. First of all, as seen in Fig. 25, there is an average true flow for intermediate impact parameters. The flow angle increases with the size of the system. Also the fluctuations reduce with increasing mass system, in agreement with Eq. (6.46) (which would indicate the absence of strong many particle correlations in INC). In large systems, like U + U, even for b = 0 the flow angle is expected to be at finite angle.[103] As the energy increases, the flow angle is expected to decrease.[102] All these considerations are consistent with a mean free path of the order of a few fm and with the angular distribution of the NN scattering.

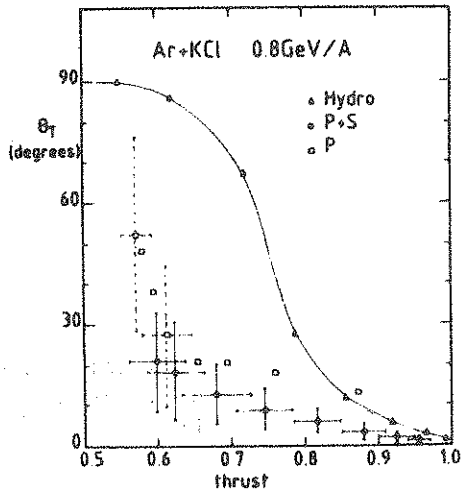

Fig. 24. Value of the thrust T and of the thrust angle ϑ_T for the Ar + KCl system at 800 MeV per nucleon and for impact parameters from 0 to 7.2 fm, as given by an INC calculation. The zero impact parameter points are on the left and the points for the largest one are on the right. The bars indicate two times the standard deviation due to the fluctuations. P means participants and S spectators. The full line gives the results of Ref. 100. The triangles correspond to the same eight impact parameters as those of the INC calculations. Taken from Ref. 102.

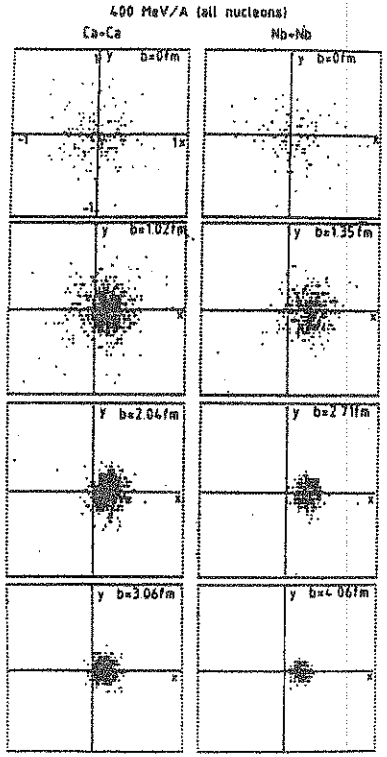

Fig. 25. Distribution of the projection of the extremity of the unit vector along the major axis of the sphericity tensor on a plane perpendicular to the beam axis, as a result of an INC calculation. See text for more detail. From Ref. 106.

Recently,[66] the first measurements of the plastic ball/wall system analyzed in terms of global variables have been presented. The dN/d cos ϑ plot shows a maximum at zero degrees for Ca + Ca at 400 MeV/A, whatever the multiplicity observed in the system. For Nb + Nb, a well-defined peak occurs in the dN/d cos ϑ plot. The corresponding angle decreases with decreasing multiplicity, disappearing for small multiplicities. The predictions of a recent INC calculation[106] are given in Fig. 26. As can be seen from the bottom of the figure, the agreement is rather good. As shown in Ref. 106, no maximum happens in Ca + Ca because fluctuations are large enough to wash out the small intrinsic flow angle. In Nb + Nb, the intrinsic flow angle is larger and the fluctuations have decreased. Furthermore, as also shown in Ref. 106, the experimental acceptance of the detector introduces a bias to large observed flow angles. Figure 27 shows the result of the hydrodynamical calculation of Ref. 63. The latter produces a definite flow when a certain relationship is assumed between the multiplicity and the impact parameter. Let us however notice that results of Fig. 27 are not corrected for the acceptance of the detector.

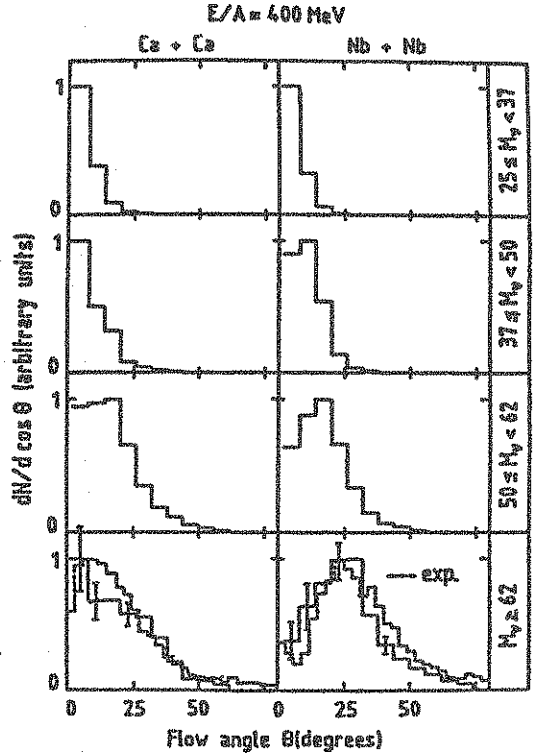

Fig. 26. Full lines : INC calculation of the dN/d cos ϑ as a functio of the multiplicity. Dotted lines : experimental data for the largest multiplicity bin.[66] Taken from Ref. 106.

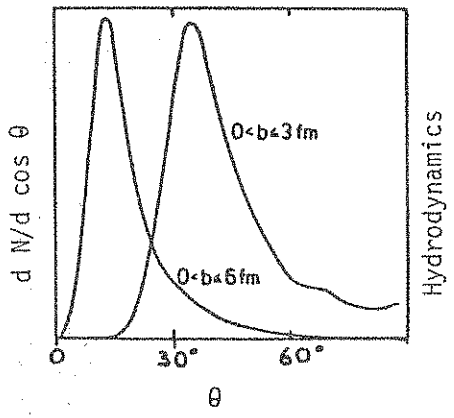

Fig. 27. dN/d cos ϑ plot for Nb + Nb at 400 MeV/A as generated by an hydrodynamical calculation. The multiplicity M_c bins are just reflecting selection on the impact parameter. Adapted from Ref. 63.

There is some uncertainty in the INC calculation,[30,66] but it seems that the INC produces a flow. The flow angle is close to experiment, a little bit too small perhaps, and definitely smaller than the hydrodynamics prediction, which seems to overshoot the experimental value. The important consequence is that with heavy systems like Nb + Nb, we start to be sensitive to the bulk dynamics. Whether this is sensitive to equation of state or the detail of NN forces requires more experimental as well as theoretical study. Work in this direction is only starting.[30,95]

7. THE SPECTATOR PHYSICS

7.1. Introduction

Although not as spectacular as the participant physics, the spectator physics nevertheless presents interesting aspects. What happens to the spectators ? Essentially, this part of the system receives an energy-momentum transfer, by far much smaller than the one suffered in the average by the participant nucleons, but sufficient anyway to split this system into fragments. The momentum spectrum of the fragments is reminescent of the initial state properties, namely of the Fermi motion. This is discussed in Section 7.2. When the spectator system is large enough, the mass spectrum of the fragments seems to follow a very simple power law. This feature is so disturbing that we postpone its discussion to the next chapter. Another interesting feature is the isospin properties. Many neutron rich isotopes can be formed in this way.[107-109] For the lack of space, we will not discuss this point. We have also to mention interesting topics, (which we will not discuss either), which are not properly pertaining to the spectator physics, but which are often discussed at the same time, presumably because experimentally they imply measurements at 0 and 180°. The first one is the backward and forward production of high-energy protons, which, as believed, are due either to a high energy tail of the Fermi motion[110] or to scattering by existing clusters,[111] although there may exist some relation between the two causes.[112] The second topic is the scaling of the pion production close to the kinematical limit. The latter was predicted by Schmidt and Blankenbecler.[113] Some deviations have been observed however.[114,115] It is not clear yet whether the scaling comes from the structure function of the nuclei or simply from phase space coming from interacting clusters.[116]

7.2. Fragment momentum spectra

One of the earliest experiment[117] performed at the Bevalac established that the fragments of ^{16}O and ^{12}C (observed at 0°) had the following distribution of parallel momentum $p_{//}$ in the projectile rest frame

$$\frac{d\sigma}{dp_{//}} \propto \exp\left(\frac{p_{//}^2}{2\sigma^2}\right) \quad . \tag{7.1}$$

The width σ depends on the mass of the fragment, is maximum for half the initial mass. To a good approximation, the dependence is parabolic : $\sigma \sim F(A - F)$, if F and A are the fragment and projectile masses, respectively. Goldhaber[118] proposed a simple explanation of these observations. He assumed that the momentum of fragment F is obtained by summing F momenta picked up at random in the Fermi distribution. The Gaussian form (7.1) results from the central limit theorem. The values of σ can be calculated as follows. If $\vec{p}_i$ is the momentum of the i^{th} nucleon, one has

$$\sum_{i=1}^{A} \vec{p}_i = 0 \quad , \tag{7.2}$$

in the projectile rest frame. Squaring this expression, one obtains

$$\sum_{i=1}^{A} \langle \vec{p}_i^{\,2} \rangle + \sum_{i \neq j}^{A} \langle \vec{p}_i . \vec{p}_j \rangle = A \langle \vec{p}_i^{\,2} \rangle + A(A-1) \langle \vec{p}_i . \vec{p}_j \rangle = 0 \tag{7.3}$$

or

$$\langle \vec{p}_i . \vec{p}_j \rangle = - \frac{1}{A-1} \langle p_i^2 \rangle \quad . \tag{7.4}$$

This last expression translates the correlation induced by the momentum conservation law. Even if the distribution of $\vec{p}_i$ is isotropic, there is some correlation between the momenta of two nucleon because the total momentum must have a fixed value. Now, for a fragment F, one has

$$\langle \left(\sum_{i=1}^{F} \vec{p}_i \right)^2 \rangle = F \langle \vec{p}_i^{\,2} \rangle + F(F-1) \langle \vec{p}_i . \vec{p}_j \rangle \quad , \tag{7.5}$$

or because of (7.4)

$$\sigma^2 = \frac{1}{3} \langle \left(\sum_{i=1}^{F} \vec{p}_i \right)^2 \rangle = \frac{1}{3} \frac{F(A-F)}{A-1} \langle \vec{p}_i^{\,2} \rangle \quad . \tag{7.6}$$

For the Fermi gas model, $\langle \vec{p}_i^{\,2} \rangle = 0.6\ p_F^2$, where p_F is the Fermi momentum, and thus, σ is related to p_F. The experiment suggests a value of $p_F \approx 220$ MeV/C, which seems smaller than the usual value.

The Goldhaber model implies momentum conservation, but does

not require energy conservation. This raises a kind of puzzle since apparently the spectator system receives an energy transfer (the energy sufficient to break up) but no momentum transfer. The transfer looks like a phonon exchange,[119] the nature of which is not understood well.[119,120] However, it is expected that the spectator system receives an impulse in the perpendicular direction.[4,121] As a result, the perpendicular momentum distribution of the fragments will be larger than the longitudinal momentum one (7.1). Noticing this difference, Hüfner et al.[122,123] have tried to extract the internal momentum distribution from the longitudinal distribution of the one-nucleon removal reactions, like $\alpha \rightarrow {}^{3}He$ or ${}^{16}O \rightarrow {}^{15}O$. The authors claim that the Hartree-Fock approximation gives a better momentum distribution, especially at high energy.[123] This looks very interesting since the high energy tail is not accessible by (e,e') or (e,e'p) experiments.

8. LIQUID-GAS PHASE TRANSITION ?

8.1. Introduction

The fragmentation of the projectile was studied in the early experiments at the Bevalac.[117] The mass yield was more or less described by the so-called abrasion-ablation model.[124] In the latter a certain number of nucleons are abraded from the projectile. The excited remnant subsequently decays by eventually emitting particles. But it was found in later experiments[125] that the mass yield in the target fragmentation region follows, for fragment masses $F \lesssim A/3$, a power law like

$$p(F) \propto F^{-\tau} \quad , \qquad (8.1)$$

where the exponent τ lies between 2 and 3. This yield is very much akin to a similar finding in nuclei bombarded with several GeV protons.[126] The authors of Ref. 126 realized that such a power law was predicted for the droplet size by Fisher's theory of condensation[127] and suggested that the observed fragmentation law signals a transition from a liquid phase to a gas phase in nuclei. Similar power laws were found[128,129] in the fragmentation resulting from heavy ion collisions between a few tens to about 200 MeV per nucleon. All these systems (spectators at high energy, nucleus after the passage of a fast proton, compound system in the Ganil regime) seem to share a common property. They are primarily excited to a few MeV per nucleon and possibly slightly compressed. Therefore, their evolution may be dominated by the nuclear equation of state for small temperatures and for densities close to ρ_0 (Chapter 1).

In Section 8.2, we are going to describe briefly an approach which encompasses the abrasion-ablation model. It is essentially based on a two regime picture and phase space considerations. In Section 8.3, we will discuss the ideas which link the fragmentation in many pieces (the so-called multifragmentation) to the equation of state.

8.2. A two-regime picture of the fragmentation

We here closely follow the presentation of Ref. 131, which gives a global view of the problem. The authors start with a detailed analysis of the mass yield of proton and light-ion induced reactions on relatively heavy targets. They arrive at the following observations : heavy fragments are produced in low-multiplicity events, whereas light ($A \lesssim 20$) ones are produced in high multiplicity events. This suggests that two regimes are alternatively at work. The first one is an *evaporation* regime, in which the spectator system just looses a few very light particles. The second one is a *multifragmentation* regime, in which the system breaks up in many pieces of the size of light nuclei. The authors of Ref. 130 propose that the parameter which determines which one of the two regimes sets is the energy per particle E_0/A deposited in the spectator system by the participant nucleons which afterwards have escaped rapidly from the system. A very convincing analysis of the scaling properties of the mass yield[130] indicates that the critical value is $E_0/A \approx 3$ MeV, a value which seems consistent with the theoretical considerations of Ref. 132. If the energy per particle of a nucleus is less than this value, it stays bound, loosing its energy by evaporation. It cannot support a higher excitation energy without breaking up. The mass yield can be calculated after the introduction of a few reasonable assumptions: (1) the number of primary NN collisions done by the participants is given by the Glauber-Matthiae rule. (2) at every NN collision, an average amount ε_0 of energy is deposited in the spectator system. The quantity ε_0 is left as a free parameter. Comparison with experiment yields $\varepsilon_0 \approx 80$ MeV in agreement with the average transverse momentum in NN collisions. (3) In the multifragmentation regime, the number of fragments is equal to the number of primary NN collisions. (4) The fragmentation is assumed to be similar to a partition of a string of length A by n random cuts. The probability of finding a fragment of mass F is

$$P_n(F) = \frac{n(n-1)}{A} \left(1 - \frac{F}{A}\right)^{n-2} \quad . \qquad (8.2)$$

An alternative statistical hypothesis is to be found in Ref. 133. The treatment of the evaporation process is quite standard.[134] With such a model, one can reproduce quite well the whole mass yield as illustrated in Fig. 28. The most important aspect of this result is that the yield in the F = 10-40 region cannot be accounted for by evaporation (at least in the present stage of its understanding) and demands the presence of another process. The detail for the region $F \lesssim 32$ is displayed in Fig. 29. The model gives almost as good results as a fit by the power law (8.1). Let us also mention that this model, which goes beyond the abrasion-ablation model (essentially by the introduction of the multifragmentation), gives

good results for the fragmentation of the projectile at high energy.

In conclusion, it seems that this model gives a reasonable description of the multifragmentation yield. It, however, does not provide any hint to the dynamical path followed by the system during the multifragmentation process.

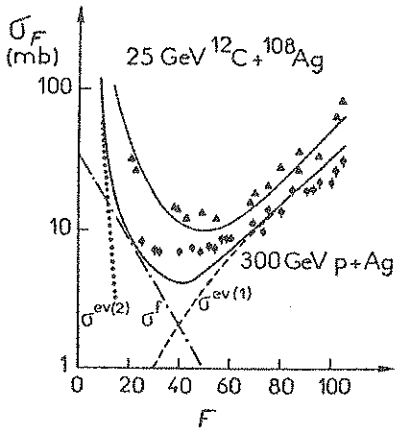

Fig. 28. Mass yield in p- and ^{12}C- Ag reactions. Data from Ref. 126. The prediction of Ref. 130 (full curve) for the p + Ag case is splitted into evaporation and multifragmentation components. Adapted from Ref. 131.

8.3. Multifragmentation and equation of state

It is known for a long time already that nuclear matter behaves like a Vanderwaals fluid,[135] i.e., that the isotherms display loops below a critical temperature T_c. This result, first obtained in the Hartree-Fock approximation[135-137] has been corroborated by more sophisticated calculations.[138,139] Without any doubt, it is due to the attractive long-ranged plus repulsive short-ranged character of the NN forces. Typically, the critical point occurs around $\rho_c \approx 0.3\ \rho_o$ and $T_c \approx 20$ MeV, as shown in Figs. 30 and 31.

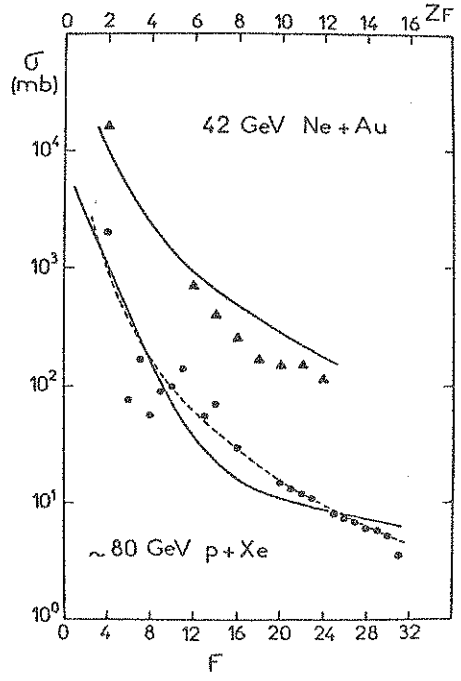

Fig. 29. Mass yield for the p + Xe and Ne-Au reactions. Data from Refs. 125, 126. The full curves are the predictions of Ref. 130 and the dashed curve is simply a fit by a power law $A^{-\tau}$, with $\tau = 2.64$. Adapted from Ref. 131.

Are the physical aspects contained in Fig. 30 relevant to the multifragmentation of a nuclear system ? For a positive answer, several conditions should be met. First, the system must be large enough to minimize surface effects, or, at least, corrections due to these effects should be approximately known. The same remark

applies to the Coulomb forces. A second condition is that the system always stays in thermal equilibrium when it is expanding. In such a case, it can be represented by a point in the (p,ρ) (or (T,ρ)) plane. Although this may be less important, one would like the concept of freeze-out to be valid. If all these conditions are met, the system is prepared in a point on the (p,ρ) plane (f.i., after two ions have stopped each other in the Ganil machine), follows a trajectory in this plane and breaks up at the end of the trajectory (the freeze-out point). This point is obviously lying on the left of the co-existence region (see Fig. 30), i.e. in the area representing the gaseous phase.

Under certain circumstances, the trajectory will cross the co-existence zone and the system will undergo a phase transition. Before being sure that such an interesting phenomenon takes place, two questions must be answered. First, what are the characteristics of the trajectory ? Second, if a liquid-gas phase transition takes place, how to detect it ? We will first consider the second question, for which an answer seems to reside in Fisher's theory[127] of condensation.

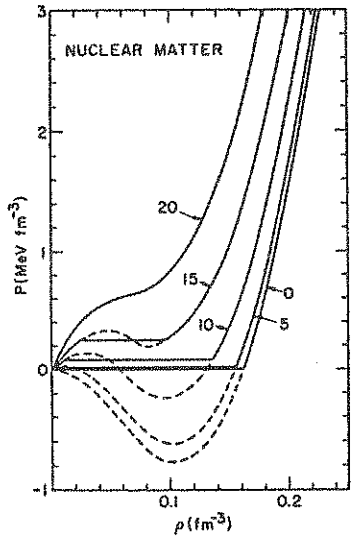

Fig. 30. Typical isotherms with the Maxwell construction (equal chemical potential) for symmetric nuclear matter (Ref. 139). The region enclosing the dotted lines is the coexistence region.

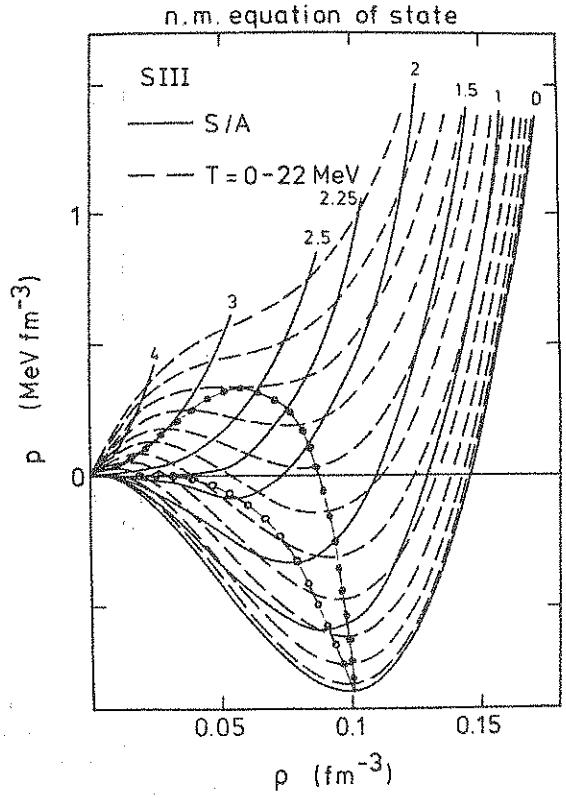

Fig. 31. Isotherms (dashed curves) and isoentropes (full curves) for symmetric nuclear matter in the Hartree-Fock-Skyrme approximation. They give the pressure p as a function of the baryon density ρ. The so-called Skyrme III force is used. The value of the entropy per nucleon is indicated for each of the isoentropes. The isotherms are given for temperatures from T = 2 (bottom) to T = 22 MeV (top) by steps of 2 MeV. The T = 0 isotherm coincides with the S/A = 0 isoentrope. The heavy dots (the spinodal curve) enclose the instability region at constant temperature whereas the open dots delineate the instability zone at constant entropy. Adapted from Ref. 144.

The basic idea of this theory, already formulated by Bijl,[140] is to consider that in the gaseous phase particles can be bound in clusters, whose average size is more and more important as the critical line (the left borderline of the coexistence zone in Fig. 30) is approached. The two main points of Fisher's theory are energy

and entropy of a cluster of size A. The energy is taken as

$$E_A = A\,E_o + w\,\sigma_A \quad , \tag{8.3}$$

where σ_A is the surface area of the cluster and where $E_o < 0$ and $w > 0$. This choice, inspired from the properties of molecular forces, is well suited to the nuclear case (which is not really surprising, since both molecular and nuclear forces are essentially attractive at long distances and repulsive at short distances). The positive surface energy favours (relatively) small surfaces. This tendancy to shrink is opposed by the entropy of the cluster which is expected to be composed of a bulk entropy and of a surface entropy

$$S_A = S_o\,A + \omega\,\sigma_A \quad .$$

The second term is a measure of the number of different configurations for a cluster of size A having a given surface area σ_A. If the temperature is lowered or if the density is increased (both correspond to an increasing activity), the entropy will be less important, the clusters will start to grow (reducing their surface) and the droplets will go to a *macroscopic* size.

The above ideas can be clothed in a more mathematical form. We start with the grand partition function for a system containing any number of cluster of species i (here $\beta^{-1} = kT$)

$$Z(V,T,\mu) = \sum_{\substack{\{N_1,N_2,\ldots\} \\ \{S_1,S_2,\ldots\}}} e^{-\beta\Sigma_i N_i E_i(S_i)}\; e^{\beta\Sigma_i \mu_i N_i}\; \frac{(g_1(S_1))^{N_1}(g_2(S_2))^{N_2}\ldots}{N_1!\;N_2!\;\ldots} \tag{8.5}$$

where S_i sums (for the moment) over all the possible states of the cluster i with a degeneracy $g_i(S_i)$. Equation (8.5) may be put in a compact form

$$Z(V,T,\mu) = \sum_{\{N_1,N_2,\ldots\}} \prod_i \frac{(q_i\,z_i)^{N_i}}{N_i!} \quad , \tag{8.6}$$

where

$$q_i = \sum_{S_i} g_i(S_i)\; e^{-\beta E_i(S_i)} \tag{8.7}$$

is the partition function for the cluster of the i^{th} type and where

$$z_i = e^{\beta\,\mu_i} \tag{8.8}$$

is the corresponding activity. The summation and product symbols in (8.6) may be interchanged, as it can easily be checked (this is a general property of different species in the grand cannonical ensemble). One then gets

$$Z(V,T,\mu) = \exp\left\{\sum_{i=1}^{\infty} q_i\,z_i\right\} \quad . \tag{8.9}$$

From this equation, one may derive the expression for the density of clusters of size A (or type i)

$$\langle N_A\rangle = \frac{\partial}{\partial\,\mu_A}\,(-\,\beta^{-1}\,\ell n\,Z) \quad , \tag{8.10}$$

or, with the help of (8.9)

$$\langle N_A\rangle = q_A\,z_A \quad . \tag{8.11}$$

These results are quite general. The originality of Fisher's theory is the introduction of an intuitive form of the partition function q_i (8.7), which satisfies however precise physical requirements. The summation over S_i in (8.7) is considered as running over the possibilities of making a surface (this is not a restriction in the case of a lattice gas). It is further assumed that all the possible manners of making a surface are very well centered on an average surface area $\overline{\sigma}_A$. Therefore (8.7) is very close to

$$q_A \approx e^{-\beta(A\,E_o + w\,\overline{\sigma}_A)}\; e^{A\,S_o + \omega\,\overline{\sigma}_A} \quad , \tag{8.12}$$

since the entropy is nothing but the logarithm of the density of states. A correction factor should be applied to (8.12) to account for all the neglected possibilities of making a surface of area $\overline{\sigma}_A$ (called as "residual entropy"). Analytical considerations force this term to be of the form $A^{-\tau}$. This term is related to the "funny shapes of a cluster (like a spaghetto) and to other combinatorial problems in self-avoiding random walks.[141] If one finally assumes that $\overline{\sigma}_A = a_o\,A^{\sigma}$, which is quite natural in nuclear physics, one finally gets

$$\langle N_i\rangle \propto x^{A^{\sigma}}\,y^{A}\,A^{-\tau} \quad , \tag{8.13}$$

with

$$x = \exp\left[-a_o\,(\beta w - \omega)\right] \quad , \tag{8.14}$$

$$y = z \exp\left[-(\beta E_o - S_o)\right] \quad . \tag{8.15}$$

The expressions (8.13-15) are obtained by assuming $\mu_A = A\mu$, $z_A = z^A$, which amounts to assume that a cluster of size A is obtained by putting together A clusters of the smallest type (the nucleons). In this case, the nucleon density is

$$\langle N \rangle = \sum_A A \langle N_A \rangle \quad . \tag{8.16}$$

Now, it is clear that the convergence rate of (8.16) is governed (see (8.13)) by the value of y. On the left of the coexistence curve, x and $y < 1$ and $\langle N_A \rangle$ decreases rapidly with A. When the coexistence curve is approached (either because the temperature drops (Eq. (8.15)) or because the chemical potential increases (Eq. (8.3)), $y \to 1$ and the $\langle N_A \rangle$ distribution decreases more slowly. If $y > 1$, the series (8.16) diverges, which physically means that very large clusters are favoured.

In Ref. 128, it is assumed that the freeze-out point is always lying on the coexistence curve as far as the freeze-out temperature T_{fo} is below the critical temperature T_c. Therefore, if $T_{fo} > T_c$, $x > 1$, $y < 1$ and the mass yield falls off more steeply than $A^{-\tau}$. At the critical point ($T_{fo} = T_c$), $x = y = 1$, the mass yield is exactly $A^{-\tau}$. Below the critical temperature, $x < 1$, $y = 1$, the mass yield falls off more steeply than $A^{-\tau}$ again. According to Ref. 128, it seems that this pattern is observed as the energy per particle increases steadily between 20 to 100 MeV/A. The authors of Ref. 128 extract the following parameters $T_c \approx 13$ MeV, $\tau \approx 1.8$ (the latter parameter is in principle related to the dimensionality of the system and to the so-called critical exponents). This success is encouraging despite of the many uncertainties that blur the analysis, namely those on the freeze-out density, on the temperature of the fragments,...

One may wonder whether the dynamical path followed by the system in the (p,ρ) plane has some influence on the multi-fragmentation itself. What is the evolution of the system once it is thermalized and possibly compressed ? The most important feature seems to be the *isoentropic* expansion of the system (Refs. 70, 142, 143 and Section 4). The system thus follows an isoentrope (full curves in Fig. 31) and not an isotherm. Along an isoentrope, the internal energy is transformed into flow motion, with a maximum efficiency : the work performed by the pressure is entirely transformed into macroscopic kinetic energy. Accordingly, the temperature of the system is decreasing.

In comparing with Figs. 20 and 31, it is already clear that the cluster formation in the participant system around 1 GeV per nucleon has little to do with the gas-liquid phase transition. The entropy per baryon of the system is too high and the isoentrope is always higher than the critical point in the (p,ρ) plane. In the Ganil regime (or in the spectator system at high energy), the system is "prepared" at a point around the upper right corner of Fig. 31. The associated isoentrope will cross the coexistence region, when followed toward small densities. Several scenarios are possible when the system reaches the coexistence curve (Fig. 30). If the evolution is sufficiently slow, the system may develop two phases (each at equal chemical potential) and evolves along the Maxwell construction. It eventually vaporizes and its composition is governed by Fisher's theory. On the other extreme, the evolution of the system may be so fast that the system does not have the time to develop two phases. It remains in the liquid phase, keeps on evolving on an isoentrope : this is the *supercooling* phenomenon. The system is then in a metastable state. In usual isothermal fluid experiments, the supercooling extends up to the spinodal curve (Fig. 31). However, here, as the expansion is at constant entropy, the supercooling may last until the encounter of the "isoentropic spinodal" (the open dots in Fig. 31), which joins all the points of vanishing $(\partial p/\partial \rho)_S$. Then the system enters the region of instability, characterized by a negative isoentropic "compressibility coefficient" $(\partial p/\partial \rho)_S < 0$. To understand the nature of this instability, let us consider an extended system with uniform particle density $\bar{\rho}$ at the top of which we add an oscillatory modification of the type

$$\rho(\vec{r}) = \bar{\rho} + a \sin(\vec{k}.\vec{r} - \omega t) \quad . \tag{8.17}$$

At this modification is associated a velocity field

$$\vec{v}(\vec{r}) = \frac{a\,\omega\,\vec{k}}{\bar{\rho}\;k^2} \sin(\vec{k}.\vec{r} - \omega t) \quad . \tag{8.18}$$

which guarantees the continuity equation. This introduces a modification in the kinetic (flow) energy

$$\delta K = \frac{M}{4\,\bar{\rho}}\, V\, \frac{a^2\,\omega^2}{k^2} \quad , \tag{8.19}$$

where V is the volume of the system (surface effects are neglected) and M is the mass of the nucleon. If H is the bulk energy density, the modification in the internal energy U is

$$\delta U = \int \left[\left(\frac{\partial H}{\partial \rho}\right)_S (\rho(\vec{r}) - \bar{\rho}) + \frac{1}{2}\left(\frac{\partial^2 H}{\partial \rho^2}\right)_S (\rho(\vec{r}) - \bar{\rho})^2 + \ldots\right] d^3r \quad . \tag{8.20}$$

Neglecting surface effects, one has in lowest (i.e. in second) order

$$\delta U = \frac{1}{4\bar{\rho}} V\left(\frac{\partial p}{\partial \rho}\right)_S a^2 \quad . \tag{8.21}$$

The theory of small oscillations tells us that the frequency ω is given by

$$\omega^2 = \frac{k^2}{M}\left(\frac{\partial p}{\partial \rho}\right)_S \quad . \tag{8.22}$$

When the derivative is negative, the frequency is imaginary. The fluctuations grow exponentially. It is suggested in Refs. 143, 144 that the multifragmentation may result from this kind of instability. However, no definite prediction has been done so far, because one is still far from having a complete dynamical theory. First, a model is needed for the expansion of a uniform hot sphere. Such a model already exists.[144,145,146] Second, the degrees of freedom associated with fluctuations like in (8.17) have to be introduced at the top of the global expansion of the system. This leads to a diffusion problem. This can be understood by looking at Fig. 32, which shows the typical variation of the internal energy of the system $U(\bar{\rho},a)$ generalized to nonuniform density by an expression like (8.17).

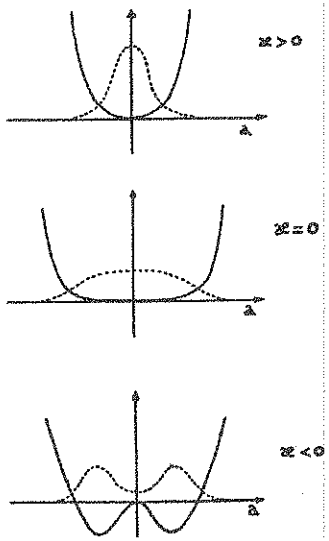

Fig. 32. Full curves : typical variation of the internal energy $U(\bar{\rho},a)$ for different values of the isoentropic compressibility coefficient $\chi = (\partial p/\partial \rho)_S$. Dotted curves : typical shapes of the distribution P(a). See text for detail.

Considered as an analytic function of a, the series expansion of U begins as (see (8.21))

$$U(\bar{\rho},a) = U(\bar{\rho}) + c_2(\bar{\rho})a^2 + c_4(\bar{\rho})a^4 + \ldots, \tag{8.23}$$

where $c_4 > 0$ and where

$$c_2(\bar{\rho}) = \frac{V}{4\bar{\rho}}\left(\frac{\partial p}{\partial \rho}\right)_S \tag{8.24}$$

has the same sign as the isoentropic compressibility coefficient. Before reaching the "isoentropic spinodal", $c_2 > 0$ and $U(\bar{\rho},a)$ has a minimum at $a = 0$. If we consider the probability P(a) of having a fluctuation of amplitude a, it will be centered at $a = 0$. Disregarding the fluctuations is probably a good approximation in this region. When $c_2 = 0$, the potential curve (8.23) opens up and as c_2 becomes more and more negative, the potential develops two pockets for two (physically equivalent) opposite values of a. As a consequence, the distribution P(a) broadens and large values of a can be obtained. Physically, it means that the fluctuations grow spontaneously, leading to "cracks" in the system. The considerations above are a simplified description of the multifragmentation as a Landau-Ginzburg[147] model of a second order phase transition whose order parameter is the amplitude a of the fluctuations itself. A more elaborate description is however needed, which would include a more general form for the fluctuation (than (8.17)) and a diffusion term for the evolution of the distribution P(a).

The most serious problem is to relate the observables, namely the mass yield to the fluctuation amplitude a. Other questions are related to the surface energy which may play a role (this is important in Fisher's theory) and to the Coulomb energy. These effects may obscure the manifestation of the bulk instability[148] (the most obvious modification is a lowering of the critical temperature to $T_c \approx 10$ MeV). However, despite the complications which soften the transition, it is very likely that multifragmentation may be due to the bulk instability. Indeed, the latter is due to attractive long ranged and repulsive short ranged forces. Even if thermodynamic concepts could not be strictly justified, it must happen situations where it is preferable for the system to exist either in a denser or in a more dilute form. This statement is supported by the recent two-dimensional Hartree calculation of Strack and Knoll.[149]

The issue is far from being settled, however. Another problem is the importance of the usual evaporation. Evidently,this process must be important when the system is excited at small pressure. Then, the system oscillates around a zero pressure state (see Fig. 31) and the only way for the system to loose energy is to emit particles.[144] However, there are indications that evaporation may be (at least partly) responsible for the multifragmentation itself.[150-152]

To conclude this section, it seems that multifragmentation happens when the system is not too much excited, but sufficiently excited for not loosing its energy by gentle evaporation. The relation between the properties of this phenomenon and the equation of state is not yet clearly established, but the actual situation seems promising.

9. CONCLUSION: OUTLOOK

From this account of the relativistic heavy ion physics, it is clear that this field is quite rich of diverse phenomena and in a phase of rapid development. Yet, the present review, supposed to be the basic material of a short series of lectures, is inevitably uncomplete. Among the topics that we did not cover, let us mention the production of strange particles, the two pion and two proton interferometry, the production of multibaryons, the production of secondary fragments with unusual mean free path (the anomalons). We did not treat these questions, either because of poor or uncertain experimental status, or because experimental data are really too scarce, or because of difficulties of interpretation. We would like however to mention the disturbing aspect of the strange particles production(K,Λ),[153-155] which seems to be produced with larger perpendicular momentum than expected,[156-160] especially the Λ's.[154] We did not discuss either the spin-isospin instability (the celebrated pion condensation) which seems to be ruled out by the present experiments.[161,162]

We are now in a situation, where the basic mechanisms of the reaction process are more or less understood. From the dozen or more models which were proposed a few years ago, only two have survived (when a simultaneous description of several aspects of the collision is needed) : the INC and hydrodynamics. Although it may not be clear from these notes, these denominations should be rather considered as generic names for two classes of closely related models. In the very recent times, the INC model is being refined to account for interaction energy. Also, there are a variety of hydrodynamic calculations (one fluid, two fluids, etc.).Both theories are designed to follow the evolution of the system in phase space. The main difference between the two approaches is twofold. First, hydrodynamics averages over local fluctuations, whereas INC keeps track of the microscopic structure all the time. Second, hydrodynamics can handle non trivial equation of state and is well suited to study the transport properties in a transparent way. Both approaches are however incomplete in the sense that they need some additional devices to treat the production of composites.

The basic mechanism can be outlined in this way. The system is divided in a more or less geometrical way into participant nucleons, which suffer large momentum transfers, and spectators which are much less perturbed. The participant system, whose mass decreases with increasing impact parameter is compressed substantially. It afterwards expands rapidly and decays into many energetic nucleons, pions and light composites. This dynamical path is largely dominated by a scheme of successive NN collisions. Due to the finite volume of the system, a few nucleons are making one or two collisions (a situation sometimes called the coronna effect). Therefore only a part of the system may be considered as in a more or less thermal equilibrium.

The ultimate goal is admittedly to extract from the observed participant properties the hadronic matter equation of state. Basically, two questions must be answered. Do we approach the bulk dynamics ? What are the observables sensitive to the equation of state ? It seems from the global analysis of the Nb + Nb data, that in this system and in heavier ones we are mainly watching the bulk dynamics at work. As for the second question, we have given in Section 6, three observables ("d"/"p" ratio, pion multiplicity, flow angle) which may be sensitive to detail of the equation of state. To our opinion, the flow angle is still too poorly determined (at least theoretically) to draw definite conclusion. The "d"/"p" ratio seems promising, but further investigation is needed. The pion multiplicity looks the most spectacular, although the interpretation of Ref. 91, which considers this quantity as a barometer, is still disputed. To our opinion, it constitutes however an obvious indication of interaction (two-body) effects. The present situation is really exciting because we feel that we are close to clearly isolate equation of state effects, even if the equation of state itself (and/or transport coefficients) would be difficult to extract because, presumably, thermodynamic concepts would be marginally applicable.

The future should probably concentrate on low energy because equation of state effects are expected to be more important in this regime. High energy (around 1 GeV/A) should not be forgotten anyway, because this region is suited to a detailed study of the mesonic properties of the matter, a topic which has not received the attention it deserves.

Paradoxically, the spectator system also provides an opportunity to study the nuclear matter equation of state, in another regime, of course. But, here too, no clear evidence of equation of state effects, a liquid-gas transition or instability in particular, is presently available and alternative (conventionally named) conventional models are also providing a good description of the data. Perhaps in this case, we do not yet have a very clear idea of the evolution of the system.

To summarize, in both cases we have indications but no evidence of equation of state effects. But we have to keep in mind that "the absence of evidence is not the evidence of absence".[163] This and the feeling that we are close to the goal will encourage us to pursue both the experimental and theoretical efforts.

ACKNOWLEDGEMENTS

I would like to express my sincere thanks to all the people with whom I had the pleasure to collaborate in this field. I would also like to thank Dr. D. Vautherin for discussions about phase transitions and Dr. X. Campi for providing me with a copy of his material before publication. I am also very grateful to Drs. B. Ascul and P. Atatras for an illuminating discussion about instability.

REFERENCES

1. The reader is assumed to be familiar with nucleus-nucleus and relativistic kinematics. If not, see, f.i. the Appendix of Ref. 4.
2. M. Lefort, this School.
3. G. Baym, "Quark Matter Conference 84", Helsinki, June 1984
4. S. Nagamiya and M. Gyulassy, Adv. Nucl. Phys. 13 (1984) 201.
5. V.I. Manko and S. Nagamiya, Nucl. Phys. A384 (1982) 475.
6. S. Nagamiya, "Quark Matter Conference 83", Brookhaven, Sept. 1983.
7. Y. Miake et al., University of Tokyo preprint, 1984.
8. S. Nagamiya, M.-C. Lemaire, S. Schnetzer, H. Steiner and I. Tanihata, Phys. Rev. Lett. 45 (1980) 602.
9. I. Tanihata, M.-C. Lemaire, S. Nagamiya and S. Schnetzer, Phys. Lett. 97B (1980) 363.
10. I. Tanihata, in : "Proceedings of Hakone Seminar on High-Energy Nuclear Interactions and Properties of Dense Nuclear Matter", K. Nakai and A.S. Goldhaber, eds., Hakone, Japan (1980), p. 382.
11. I. Tanihata, S. Nagamiya, S. Schnetzer and H. Steiner, Phys. Lett. 100B (1981) 121.
12. S. Nagamiya et al., Phys. Rev. C24 (1981) 971.
13. J. Cugnon, T. Mizutani and J. Vandermeulen, Nucl. Phys. A352 (1981) 505.
14. J. Cugnon, D. Kinet and J. Vandermeulen, Nucl. Phys. A379 (1982) 553.
15. P.J. Siemens and J.O. Rasmussen, Phys. Rev. Lett. 42 (1979) 844.
16. G. Bertsch, in : "Progress in Particle and Nuclear Physics" vol. 4, D. Wilkinson, ed., Pergamon, Oxford (1980), p. 483.
17. P. Danielewicz, Ann. Phys. 152 (1984) 239, 305.
18. R. Yvon, "Les Corrélations et l'Entropie Statistique Classique", Dunod, Paris (1965).
19. P.C. Martin and J. Schwinger, Phys. Rev. 115 (1959) 1342.
20. E.P. Wigner, Phys. Rev. 40 (1932) 749.
21. S.E. Koonin, in "Nuclear Theory 1981", ed. by G. Bertsch, WSPC, 1982.
22. L.P. Kadanoff and G. Baym, "Quantum Statistical Mechanics", Benjamin, New York (1962).
23. J. Cugnon, Nucl. Phys. A387 (1982) 191c.
24. R. Balescu, "Equilibrium and Non Equilibrium Statistical Mechanics", Wiley-Interscience, New York (1975), ch. 11.
25. A.R. Bodmer and A.D. MacKeller, Phys. Rev. C15 (1977) 1342.
26. L. Wilets, Y. Yariv and R. Chesnut, Nucl. Phys. A301 (1978) 359.
27. D.J.E. Callaway, L. Wilets and Y. Yariv, Nucl. Phys. A327 (1979) 250.
28. A.R. Bodmer, C.N. Panos and A.D. MacKeller, Phys. Rev. C22 (1980) 1025.
29. A.R. Bodmer and C.N. Panos, Nucl. Phys. A356 (1981) 517.
30. J.J. Molitoris et al., MSU preprint (1984).
31. J. Randrup, Nucl. Phys. A316 (1979) 509.
32. H.J. Pirner and B. Schürmann, Nucl. Phys. A316 (1979) 461.
33. B. Schürmann, Phys. Rev. C20 (1979) 1607.
34. B. Schürmann and N. Mancoc-Borstnik, Phys. Rev. C26 (1982) 519.
35. R. Malfliet, Phys. Rev. Lett. 44 (1980) 864.
36. R. Malfliet, Nucl. Phys. A363 (1981) 429 ; 456.
37. J. Cugnon, Phys. Rev. C23 (1981) 2094.
38. R.L. Hatch and S.E. Koonin, Phys. Lett. 81B (1978) 1.
39. B. Schürmann and J. Randrup, Phys. Rev. C23 (1981) 2766.
40. J. Hüfner and J. Knoll, Nucl. Phys. A290 (1977) 460.
41. J. Knoll and J. Randrup, Nucl. Phys. A324 (1979) 445.
42. J. Knoll and J. Randrup, Phys. Lett. 103B (1981) 264.
43. J. Cugnon, J. Knoll and J. Randrup, Nucl. Phys. A360 (1981) 444.
44. J. Knoll, Phys. Rev. C20 (1979) 773.
45. S. Bohrmann and J. Knoll, Nucl. Phys. A356 (1981) 498.
46. A.H. Blin, S. Bohrmann and J. Knoll, Z. Physik A306 (1982) 177.
47. K.K. Gudima and V.D. Toneev, Yad. Fiz. 27 (1978) 658 [Sov. J. Nucl. Phys. 27 (1978) 351].
48. E.C. Halbert, Phys. Rev. C23 (1981) 295.
49. H. Stöcker, J. Hofmann, J.A. Maruhn and W. Greiner, Prog. Part. Nucl. Phys. 4 (1980) 133.
50. J. Cugnon and J. Vandermeulen, in : "Winter College on Nuclear Physics", Trieste, March 1984.
51. G. Bertsch and G. Baym, to be published.
52. A.A. Amsden, G.F. Bertsch, F.H. Harlow and J.R. Nix, Phys. Rev. Lett. 35 (1975) 905.
53. A.A. Amsden, F.H. Harlow and J.R. Nix, Phys. Rev. C15 (1977) 1059.
54. C.F. Chapline, H.H. Johnson, E. Teller and M.S. Weiss, Phys. Rev. D8 (1973) 4302.
55. L.D. Landau and E.M. Lifshitz, "Fluid Mechanics", Pergamon, Oxford (1959).
56. H. Stöcker, M.Gyulassy and J. Boguta, Phys. Lett. 103B (1981) 269.
57. J.R. Nix, Progr. Part. Nucl. Phys. 2 (1979) 237.
58. P. Danielewicz, unpublished.
59. H. Stöcker et al., Phys. Rev. Lett. 47 (1981) 1807.
60. G. Buchwald, L.P. Csernai, J.A. Maruhn and W. Greiner, Phys. Rev. C24 (1981) 135.
61. A. Sandoval et al., Phys. Rev. C21 (1980) 1321.
62. J.R. Nix and D. Strottman, Phys. Rev. C23 (1981) 2548.
63. G. Buchwald et al., Phys. Rev. Lett. 52 (1984) 1594.
64. H.H.K. Tang and C.Y. Wong, Phys. Rev. C21 (1980) 1846.
65. R. Stock et al., Phys. Rev. Lett. 44 (1980) 1243.
66. H.A. Gustafsson et al., Phys. Rev. Lett. 52 (1984) 1590.

67. H.H. Gutbrod et al., Phys. Rev. Lett. 37 (1976) 667.
68. M.-C. Lemaire et al., Phys. Lett. 85B (1979) 38.
69. M.-C. Lemaire, in "Proceedings of the 2nd French-Japanese Colloquium on Nuclear Physics with Heavy Ions", IN2P3 Publication, Gif-Sur-Yvette, France (October, 1979) p. 139 [Preprint : Lawrence Berkeley Laboratory Report LBL-10555 (1979)].
70. G. Bertsch and J. Cugnon, Phys. Rev. C24 (1981) 2514.
71. E.A. Remler, Ann. Phys. (N.Y.) 136 (1981) 293.
72. E.A. Remler, Phys. Rev. C25 (1982) 2974.
73. S.F. Butler and C.A. Pearson, Phys. Rev. 129 (1963) 836.
74. M. Gyulassy, K. Frankel and E.A. Remler, Nucl. Phys. A402 (1983) 596.
75. S. Nagamiya, in : "Proceedings of the Symposium on Heavy Ion Physics from 10 to 200 MeV/A", Brookhaven 1979. See also Ref. 61.
76. P.J. Siemens and J.I. Kapusta, Phys. Rev. Lett. 43 (1979) 1486.
77. H. Stöcker, Lawrence Berkeley Laboratory Report LBL-12302 (1981).
78. J. Knoll, L. Münchow, G. Röpke and H. Schulz, Phys. Lett. 112B (1982) 13.
79. H. Sato and K. Yazaki, Phys. Lett. 98B (1981) 153.
80. H.H. Gutbrod et al., Nucl. Phys. A397 (1982) 177c.
81. S. Nagamiya, in : "Proceedings of the International Conference on Nuclear Physics", P. Blasi and R.A. Ricci, eds., Tipografia Compositori, Bologna (1983), p. 431.
82. G. Bertsch and J. Cugnon, unpublished.
83. A.Z. Mekjian, Phys. Rev. C17 (1978) 1051.
84. J.I. Kapusta, Phys. Rev. C16 (1977) 1493.
85. J. Gosset, J.I. Kapusta and G.D. Westfall, Phys. Rev. C18 (1978) 844.
86. J. Randrup and S.E. Koonin, Nucl. Phys. A356 (1981) 223.
87. G. Fái and J. Randrup, Nucl. Phys. A381 (1982) 557.
88. A. Sandoval et al., Phys. Rev. Lett. 45 (1980) 874.
89. J.J. Lu et al., Phys. Rev. Lett. 46 (1981) 898.
90. M. Gyulassy and S.K. Kauffmann, Phys. Rev. Lett. 40 (1978) 298.
91. R. Stock et al., Phys. Rev. Lett. 49 (1982) 1236.
92. J.W. Harris and R. Stock, in : "7th Oaxtepec Meeting on Nuclear Physics" (January 1984).
93. M. Cahay, J. Cugnon and J. Vandermeulen, Nucl. Phys. A411 (1983) 524.
94. G. Bertsch, H. Kruse and S. Das Gupta, Phys. Rev. C29 (1984) 673.
95. R. Malfliet, KVI preprint (1984).
96. R. Malfliet, Nucl. Phys. A420 (1984) 621.
97. D. Enskog, Kugl. Svenska Vet. Akad. Handl. 63 (1921) n° 4.
98. H. Pirner, Phys. Rev. C22 (1980) 1962.
99. G. Bertsch and A.A. Amsden, Phys. Rev. C18 (1978) 1293.
100. J. Kapusta and D. Strottman, Phys. Lett. 106B (1981) 33.
101. J. Cugnon, J. Knoll, C. Riedel and Y. Yariv, Phys. Lett. 109B (1982) 167.
102. J. Cugnon and D. L'Hôte, Nucl. Phys. A397 (1983) 519.
103. M. Gyulassy, K.A. Frankel and H. Stöcker, Phys. Lett. 110B (1982) 185.
104. H. Stöcker et al., Phys. Rev. C25 (1982) 1873.
105. P. Danielewicz and M. Gyulassy, Phys. Lett. 129B (1983) 283.
106. J. Cugnon and D. L'Hôte, Phys. Lett. (in press).
107. T.J.M. Symons et al., Phys. Rev. Lett. 42 (1979) 40.
108. G.D. Westfall et al., Phys. Rev. Lett. 43 (1979) 1859.
109. P.B. Price and J. Stevenson, Phys. Rev. C24 (1981) 2101.
110. S. Frankel and R.M. Woloshyn, Phys. Rev. C16 (1977) 1680.
111. T. Yukawa and S. Furui, Phys. Rev. C20 (1979) 2316.
112. O.Bohigas and S. Stringari, Phys. Lett. 95B (1980) 9.
113. I.A. Schmidt and R. Blankenbecler, Phys. Rev. D15 (1977) 3321 ; Phys. Rev. D16 (1977) 1318.
114. L.S. Schroeder et al., Phys. Rev. Lett. 43 (1979) 1787.
115. R.H. Landau and M. Gyulassy, Phys. Rev. C19 (1979) 149.
116. J. Knoll and S. Shyam, G.S.I. Preprint (1984).
117. D.E. Greiner et al., Phys. Rev. Lett. 35 (1974) 152.
118. A.S. Goldhaber, Phys. Lett. 53B (1974) 306.
119. H. Feshbach and K. Huang, Phys. Lett. 47B (1973) 300.
120. H. Feshbach and M. Zabek, Ann. Phys. 107 (1977) 110.
121. C.A. Whitten, Jr., Nucl. Phys. A335 (1980) 419.
122. T. Fujita and J. Hüfner, Nucl. Phys. A343 (1980) 493.
123. J. Hüfner and M.C. Nemes, Phys. Rev. C23 (1981) 2538.
124. J. Hüfner, K. Schafer and B. Schürmann, Phys. Rev. C12 (1975) 1888.
125. A.I. Warwick et al., Phys. Rev. C27 (1983) 1083.
126. N. Porile et al., Phys. Rev. C19 (1979) 2288.
127. M.E. Fisher, Physics 3 (1967) 225.
128. A.D. Panagiotou et al., Phys. Rev. Lett. 52 (1984) 496.
129. Y. Cassagnou et al., preprint Saclay 2151, April 1984.
130. X. Campi, J. Desbois and E. Lipparini, Phys. Lett. 142B (1984) 8.
131. X. Campi, J. Desbois and E. Lipparini, in : "Heavy Ion Conference", Paris, May 1984.
132. G. Bertsch and D. Mundinger, Phys. Rev. C17 (1977) 1646.
133. J. Aichelin and J. Hüfner, Phys. Lett. 136B (1984) 15.
134. X. Campi and J. Hüfner, Phys. Rev. C24 (1981) 2199.
135. M. Brack and P. Quentin, Phys. Lett. B52 (1974) 159.
136. U. Mosel, P.G. Zint and K.H. Passler, Nucl. Phys. A236 (1974) 252.
137. G. Röpke, L. Münchow and H. Schulz, Phys. Lett. 110B (1982) 21.
138. M. Barranco and J.R. Büchler, Phys. Rev. C22 (1980) 1729.
139. B. Friedman and V.R. Pandharipande, Nucl. Phys. A361 (1981) 502.
140. A. Bijl, Thesis, Leiden (1938).
141. M.E. Fisher and M.F. Sykes, Phys. Rev. 114 (1959) 45.
142. M.I. Sobel, P.J. Siemens, J.P. Bondorf and H.A. Bethe, Nucl. Phys. A251 (1975) 502.
143. G. Bertsch and P.J. Siemens, Phys. Lett. 126B (1983) 9.
144. J. Cugnon, Phys. Lett. 135B (1984) 374.
145. J.P. Bondorf, S.I.A. Garpmann and J. Zimanyi, Nucl. Phys. A296

(1978) 320.
146. M.W. Curtin, H. Toki and D.K. Scott, Phys. Lett. 123B (1983) 289.
147. V.L. Ginzburg and L.D. Landau, Zh. Eksp. Teor. Fiz. 20 (1950) 1064.
148. P. Bonche, S. Levit and D. Vautherin, Nucl. Phys. (in press).
149. B. Strack and J. Knoll, Z. Physik A315 (1984) 249.
150. P. Bonche, S. Levit and D. Vautherin, Saclay preprint (1984).
151. W.A. Friedman and W.G. Lynch, Phys. Rev. C28 (1983) 950.
152. D.H. Boal, preprint MSUCL-451 (1984).
153. S. Schnetzer et al., Phys. Rev. Lett. 49 (1982) 989.
154. J.W. Harris et al., Phys. Rev. Lett. 47 (1981) 229.
155. A. Shor et al., Phys. Rev. Lett. 48 (1982) 1597.
156. J. Randrup and C.M. Ko, Nucl. Phys. A343 (1980) 519.
157. W. Zwermann et al., Phys. Lett. 134B (1984) 392.
158. J. Cugnon and R. Lombard, Nucl. Phys. A422 (1984) 635.
159. J. Randrup, Phys. Lett. 99B (1981) 9.
160. S. Nagamiya, Phys. Rev. Lett. 49 (1982) 1383.
161. M. Gyulassy, Nucl. Phys. A354 (1981) 395.
162. S. Nagamiya et al., Phys. Rev. Lett. 48 (1982) 1780.
163. C. Sagan, "The Dragons of Eden", Ballantine Books, New York (1977).